Integration of system phenotypes in microbiome networks to identify candidate synthetic communities: a study of the grafted tomato rhizobiome

Ravin Poudel[1234#], Ari Jumpponen[5], Megan M. Kennelly[4], Cary Rivard[6], Lorena Gomez-Montano[1234], and Karen A. Garrett[1234#].

[1]*Department of Plant Pathology, University of Florida, Gainesville, FL 32611*
[2]*Global Food Systems Institute, University of Florida, Gainesville, FL 32611*
[3]*Emerging Pathogens Institute, University of Florida, Gainesville, FL 32611*
[4]*Department of Plant Pathology, Kansas State University, Manhattan, KS 66506*
[5]*Division of Biology and Ecological Genomics Institute, Kansas State University, Manhattan, KS 66506*
[6]*Department of Horticulture and Natural Resources, Kansas State University, Olathe, KS 66061*

[#]*Correspondence: Ravin Poudel and Karen A. Garrett*
E-mail addresses: rp3448@ufl.edu and *karengarrett@ufl.edu*

Running title: Phenotype-based networks for microbial consortia design

ABSTRACT

Understanding factors influencing microbial interactions, and designing methods to identify key taxa, are complex challenges for achieving microbiome-based agriculture. Here we study how grafting and the choice of rootstock influence root-associated fungal communities in a grafted tomato system. We studied three tomato rootstocks (BHN589, RST-04-106 and Maxifort) grafted to a BHN589 scion and profiled the fungal communities in the endosphere and rhizosphere by sequencing the Internal Transcribed Spacer (ITS2). The data provided evidence for a rootstock effect (explaining ~2% of the total captured variation, $p < 0.01$) on the fungal community. Moreover, the most productive rootstock, Maxifort, supported greater fungal species richness than the other rootstocks or controls. We then constructed a phenotype-OTU network analysis (PhONA) using an integrated machine learning and network analysis approach based on sequence-based fungal Operational Taxonomic Units (OTUs) and associated tomato yield data. PhONA provides a graphical framework to select a testable and manageable number of OTUs to support microbiome-enhanced agriculture. We identified differentially abundant OTUs specific to each rootstock in both endosphere and rhizosphere compartments. Subsequent analyses using PhONA identified OTUs that were directly associated with tomato fruit yield, and others that were indirectly linked to yield through their links to these OTUs. Fungal OTUs that are directly or indirectly linked with tomato yield may represent candidates for synthetic communities to be explored in agricultural systems.

IMPORTANCE

The realized benefits of microbiome analyses for plant health and disease management are often limited by the lack of methods to select manageable and testable synthetic microbiomes. We evaluated the composition and diversity of root-associated fungal communities from grafted tomatoes. We then constructed a phenotype-OTU network analysis (PhONA) using these linear and network models. By incorporating yield data in the network, PhONA identified OTUs that were directly predictive of tomato yield, and others that were indirectly linked to yield through their links to these OTUs. Follow-up functional studies of taxa associated with effective rootstocks, identified using approaches like PhONA, could support the design of synthetic fungal communities for microbiome-based crop production and disease management. The PhONA framework is flexible for incorporation of other phenotypic data and the underlying models can readily be generalized to accommodate other microbiome or other 'omics data.

KEYWORDS

fungi, phenotypes, microbiome networks, model integration, grafting, tomato

54 **Introduction**

55 Interactions are key to defining system behaviors, structures, and outcomes. In microbial systems,
56 interactions among organisms define their distribution, assemblies, and ecosystem functions. In
57 addition to microbe-microbe interactions, microbes interact with their hosts, and are essential to
58 host health and performance (1-8). In agriculture, plant–microbe interactions improve plant
59 productivity by providing access to nutrients (9-11), reducing infection by plant pathogens (5, 12),
60 triggering plant growth promoting factors (13, 14), and enhancing plant resistance (15, 16) and
61 tolerance to abiotic stresses (17-19). Although the importance of microbes and host-microbe
62 interactions to host health and ecological processes is well-known, interaction-based approaches to
63 manage crop-production remain a scientific frontier. Past attempts to translate information about
64 microbial interactions to design biocontrol agents or biofertilizers have often had limited efficacy
65 and durability (20, 21). Most microbial inocula have been applied as single species, often selected
66 based on pairwise relations of microbes with a pathogen or the host. Interactions among microbes
67 as well as with the host are important, and the net outcome of these complex interactions defines
68 host health and ecosystem functions(22). Thus, it is critical to understand the ecology of microbes
69 selected for biological applications, and systems approaches centered on host-microbe interaction
70 can help guide the selection of microbes for synthetic communities(23).

71 Among tools to better understand microbial interactions, network models of microbial
72 communities, and studies of network structures and key groups, have proven popular for generating
73 hypotheses about how to engineer microbial consortia. In such network models of microbiomes, a
74 node represents an OTU, and a link exists between two OTUs if their sequence proportions are
75 significantly associated across samples. When evaluated with other conventional measures of
76 microbial community structures, such as diversity indices, network models can be used to identify
77 hub taxa that may be key to maintaining microbial assemblages and diversity (24), or to evaluate
78 changes in community complexity and interactions in response to experimental treatments (25).
79 Microbiome networks are useful for describing general community structures and their key
80 properties and are often the most practical option when additional information about species
81 interactions is missing or the goal is to compare across studies with different types of data (26, 27).
82 The utility of network analysis for identifying candidate assemblages for biocontrol can be enhanced
83 by incorporating nodes that represent other additional types of features (28, 29). For instance, a
84 novel association of host metadata with the microbiome was revealed in an integrated microbiome-
85 metadata network (30), where a feature strongly associated with hub microbes can serve as a marker

86 to measure host performance. In agriculture, plant yield or other phenotypic traits can be integrated
87 in microbiome networks, with the potential to identify microbial consortia that are predictive of host
88 phenotypes. Because such models include host phenotypes, they facilitate finding candidate sets of
89 OTUs that may directly or indirectly affect host phenotypic traits. Visualization of networks is often
90 valuable for this purpose, but the real value of phenotype-based network models is their ability to
91 infer potential candidate taxa or consortia. The hypothesized beneficial sets of OTUs may represent
92 targets for pure culturing efforts or, if cultures exist, the sets can be further evaluated in laboratory
93 or field studies.

94 While phenotype-based network models have the potential to identify key taxa, application
95 of such models should be integrated with findings from other community analyses so that the
96 inference about key taxa is biologically and ecologically meaningful. For example, plant microbiome
97 studies indicate that a small but consistent proportion of variation in microbial communities is often
98 explained by the host genotype (31-37), indicating the potential for genotype-based modulation of
99 microbial communities in crop-production on a broader scale. These results support the idea of
100 host-specific microbial community selection (38). Many such microbes may be taxa that are
101 evolutionarily essential for the survival and function of plants (39, 40). In addition, the extent of host
102 genotype filtering of microbes differs across the rhizosphere, rhizoplane, and endosphere, and varies
103 from one host species to another (41-43). Results that indicate microbial filtering by different crop
104 hosts, plant compartments, geographic locations, and environmental factors (44, 45) are promising
105 for designing experiments to minimize the search space, or necessary sample numbers, to identify
106 candidate taxa for synthetic communities. For instance, factors that explain great variation in
107 microbial community composition, but that are outside the control of management, can be treated
108 as blocks in experimental designs, so that host- or compartment-specific effects on the microbial
109 community can be searched to identify the most desirable candidate taxa.

110 In our current study, building on previously described agricultural experiments in grafted
111 tomato systems (46, 47), we characterized the root-associated fungal (RAF) communities and
112 implemented an interaction-based approach to select potential candidate fungi that are predictive of
113 tomato yield and/or that are in significant association with other fungal taxa. The new phenotype-
114 OTU network analysis (PhONA) is a method for network-visualization and a framework to support
115 the selection of candidate taxa and to integrate system traits (such as host yield) in microbe-microbe
116 association networks. PhONA first identifies OTUs predictive of phenotype using lasso regression,
117 then uses the predicted OTUs from lasso regression to build a reduced GLM. PhONA then

118 combines the GLM results indicating positive or negative associations of the predicted OTUs with
119 the host phenotype as well as with other OTUs in a network model (Fig. 1). Due to the large
120 number of OTUs compared to the sample size, lasso regression was used because it is suited for
121 minimizing overfitting when applied with a relatively small sample size (48) and has been
122 implemented in microbiome studies (49, 50).

123 Phenotype-based selection of microbial consortia is promising as an effective approach to
124 select representative microbial taxa and could support the design of microbiome-based products.
125 Changes in abundance (51), successive selection over multiple generations (3), or analyses of binary
126 host-microbe relationships (52) are some of the recent phenotype-based applications to select
127 candidate taxa for biological applications. Despite the importance of biological test-based
128 approaches, difficulty in culturing all the microbes makes computational approaches instrumental to
129 define microbe-microbe and host-microbiome associations, and to identify the biological and
130 ecological key taxa. Tools to describe the community structures based on the co-occurrence matrix
131 or covariance structures (53, 54) are more common, whereas tools to integrate host phenotype or
132 environmental factors are at an earlier phase of development. Relatively small sample sizes
133 combined with large number of features may limit applications of the recent graph-based
134 approaches. Such methods allow measurement of direct associations via conditional dependence
135 structures and offer options to include environmental and phenotypic information in the model (55).
136 CoNet (56) and Flashweave (55) allow representation of the phenotype or an environmental variable
137 as an extra node or a column in the adjacency matrix, and the same statistical method can be applied
138 to define the associations among microbes and between microbes and phenotypes (taxa and
139 metadata). PhONA is generic as it allows the user to select data structure-specific models for
140 microbe-microbe and microbe-phenotype associations.

141 In the current case study, we used lasso regression to identify the subset of OTUs and then
142 fitted them using GLMs to predict OTU-phenotype associations, whereas the OTU-OTU
143 associations were defined using SparCC. Additionally, we contrasted the RAF community's diversity
144 and interactions among the rootstocks and the controls, for endosphere and rhizosphere
145 compartments. Based on our yield data, rootstock vigor, and previous studies of microbial
146 interactions (25), we expected a greater number of fungal OTUs and of microbial associations for
147 more productive rootstocks. Moreover, in our previous studies of bacterial communities in the
148 tomato rhizobiome, we observed compartment-specific (endosphere vs rhizosphere) effects of
149 grafting and rootstocks on bacterial community composition and diversity (47), and expected similar

150 effects on RAF diversity and composition. All the code and vignettes for PhONA are available at
151 https://ravinpoudel.github.io/PhONA/index.html and archived at zenodo (DOI:
152 10.5281/zenodo.6600986).
153
154
155 **METHODS**
156 **Experimental Plots, Rootstocks, and Study Sites.** We studied grafted tomato plants in
157 high tunnels in an experimental design similar to that described by Poudel et al. (47). Tomato plants
158 were grafted following a tube-grafting protocol described in Meyer et al. (46). Our study included
159 three rootstocks (BHN589; RST-04-106, and Maxifort) in four graft treatments: 1) nongrafted
160 BHN589 plants; 2) selfgrafted BHN589 plants (plants grafted to their own rootstock); 3) BHN589
161 grafted to RST-04-106; and 4) BHN589 grafted to Maxifort. We chose BHN589 as scion primarily
162 based on its popularity due to high yield and high-quality fruit with a long shelf life. For rootstocks,
163 we selected Maxifort because it is a productive and popular rootstock, and RST-04-106 as a new
164 rootstock variety based on tomato breeders' recommendations.
165 Our study included two sites: Olathe Horticulture Research and Extension Center (OHREC)
166 and Common Harvest Farm, a farm managed by a collaborating farmer. For more information
167 about the sites, see Table S1. At each study site, the four graft treatments were assigned to four plots
168 per block in a randomized complete block design. Each plot consisted of 5-8 plants, and one middle
169 plant per plot was sampled during the peak growth stage. There were six blocks at OHREC, and
170 four blocks at Common Harvest Farm, such that for each year, each graft treatment was replicated
171 10 times. The experiment was repeated for two years (2014 and 2015) with a similar design, with the
172 blocks and rootstocks randomly and independently assigned in each year.
173 **Sample Preparation, DNA Extraction, and Amplicon Generation.** To compare the
174 fungal communities, we selected a center plant from each plot and carefully dug the whole plant out
175 such that the majority of the roots remained intact. Endosphere and rhizosphere samples were
176 prepared as previously described (47) and the total genomic DNA was extracted using a DNA
177 extraction kit (MoBio UltraClean Soil DNA Isolation Kit; MoBio, Carlsbad, CA, USA) as per
178 manufacturer's protocol, with slight modification during the homogenization step (47). To recover
179 high genetic diversity, we opted for the two-step PCR approach. The primary PCR amplicons were
180 generated in 50 μL reactions under the following conditions: 1 μM forward and reverse primers, 10
181 ng template DNA, 200 μM of each dioxynucleotide, 1.5 mM $MgCl_2$, 10 μL 5x Phusion Green HF

182 buffer (Finnzymes, Vantaa, Finland), 24.5 µL molecular biology grade water, and 1-unit (0.5 µL)
183 Phusion Hot Start II DNA Polymerase (Finnzymes, Vantaa, Finland). PCR cycle parameters
184 consisted of a 98° C initial denaturing step for 30 seconds, followed by 30 cycles at 98° C for 10
185 seconds, 57° C annealing temperature for 30 seconds, and 72° C extension step for 30 seconds,
186 followed by a final extension step at 72° C for 10 minutes. All samples were PCR-amplified in
187 triplicate to minimize stochasticity, pooled, and cleaned using Diffinity RapidTip (Diffinity
188 Genomics, West Chester, PA, USA). In this PCR, we amplified the entire ITS region of fungal
189 rRNA genes using primers ITS1F-CTTGGTCATTTAGAGGAAGTAA and ITS4-
190 TCCTCCGCTTATTGATATGC (e.g. 57). The average amplicon length of the ITS region in fungi
191 is about 600 bp and could not reliably be fully covered with the Illumina MiSeq platform (v.3-
192 chemistry) in a single read. Thus, in the following nested PCR, only ITS2 of the ITS region was
193 amplified using fITS7-ITS4 primers (58) incorporating unique Molecular Identifier Tags (MIDs) at
194 the 5' end of the reverse primer (ITS4). For the nested PCR, we used similar reagents and PCR
195 conditions as in the primary PCR, with some modifications: the number of PCR cycles was reduced
196 to ten, total reaction volume was reduced to 25 ul, and 5 ul of cleaned PCR product from the first
197 PCR amplification was used as the DNA template. The nested PCR was also run in triplicate, pooled
198 by experimental unit, and cleaned with an Agencourt AmPure cleanup kit using a SPRIplate 96-ring
199 magnet (Beckman Coulter, Beverly, MA, USA) as per the manufacturer's protocol. Then, 200 ng of
200 cleaned, barcoded amplicons were combined per experimental unit, and the final pool was cleaned
201 again using an Agencourt AmPure cleanup kit as above. Illumina MiSeq adaptors were ligated to the
202 library and paired-end sequenced on a MiSeq Personal Sequencing System (Illumina, San Diego, CA,
203 USA) using MiSeq Reagent Kit V3 with 600 cycles. The endosphere and the rhizosphere amplicon
204 libraries were sequenced separately in two runs. Adaptor ligation and sequencing were performed at
205 the Integrated Genomics Facility at Kansas State University. All sequence data generated in this
206 study were deposited in the NCBI Sequence Read Archive depository (BioProject:……).
207 **Bioinformatics and OTU Designation.** The sequence library of fastq files was curated
208 using the MOTHUR pipeline (Version 1.33.3; (59)) following steps modified from the MiSeq
209 Standard Operating Protocol (SOP; www.mothur.org/wiki/MiSeq_SOP). Briefly, the forward and
210 the reverse reads were assembled into contigs using the default alignment algorithm. Any sequences
211 shorter than 250 base pairs or containing an ambiguous base call or more than eight homopolymers
212 or missing MIDs were removed from the library. Barcoded sequences were assigned to experimental
213 units, and the data for endosphere and rhizosphere libraries were merged and processed together for

214 the remaining steps in the MOTHUR pipeline. The pairwise distance matrix based on the filtered
215 sequences was created and sequence data clustered into OTUs at 97% sequence similarity using the
216 nearest neighbor joining algorithm. The clustered OTUs were assigned to a putative taxonomic
217 identity using a Bayesian classifier (60) referencing the UNITE plus INSD non-redundant ITS
218 database (61). To minimize the bias resulting from unequal sequence counts per sample, samples
219 were rarified to the lowest sequence count among the samples (6,777). The final curated OTU
220 database included 1,084,281 total sequences representing 16,151 fungal OTUs, including singletons
221 (5,376).

222 **Statistical analyses.** We evaluated the network of associations among fungal OTUs with
223 network models to better understand the community composition and the interactions therein. The
224 observed OTU database was divided into eight subsets, each combination of the four rootstocks and
225 two compartments (endosphere and rhizosphere), such that we constructed eight networks in total.
226 In our network models, a node represents an OTU and a link exists between a pair of OTUs if there
227 is evidence ($p < 0.05$) that their frequencies are correlated (positively or negatively) across samples.
228 Reducing false associations due to compositional bias in network modeling of microbiome data is
229 important for clearer interpretation (62). Thus, we used a Sparse Correlations for Compositional
230 data (SparCC) method to evaluate the pairwise associations (62), designed to minimize the
231 compositional bias effect due to normalization. In our analyses, associations were defined in 20
232 iterations, and the significance of a pairwise association was determined from 100 bootstrapped
233 datasets. Once the matrix defining all the pairwise associations was derived, we selected only those
234 OTUs for which the absolute value of at least one association was greater than 0.5 (and $p < 0.05$) in
235 the network analyses for each of the rootstock genotypes.

236 To identify the OTUs associated with tomato yield in each rootstock, a regression-based
237 model was fitted to the observed data. Marketable tomato yield data reported by Meyer et al. (46)
238 was the response variable and fungal OTUs were potential predictors. We used the caret package
239 (63) to evaluate the lasso regression and selected OTUs using varImp functions. Lasso regression
240 used an L1 regularization approach to shrink the less important variables' coefficients to zero and to
241 reduce the number of variables in the model. In lasso regression, lambda determines the penalty of
242 regularization, and its value can range from zero to infinity; when it is zero, the results are similar to
243 the least square lines. A grid-based approach was used to tune the lambda parameter using repeated
244 (ITERS=500) 5-fold cross-validation and the value of lambda with lowest variance was selected.
245 Only the OTUs with non-zero coefficients were selected, based on the lasso-regression model, to

246 build the reduced GLM model, and the association type of each OTU with phenotype was
247 estimated. Given the small sample size, we did not evaluate the model performance by splitting the
248 data into training and test cases, although this would be a valuable step in future studies with larger
249 sample sizes. PhONA then integrates the results from the GLM model for yield with the OTU-
250 OTU association network. We plotted the resulting network using the igraph package (54) in R. To
251 evaluate the role of nodes in the network, we placed each node in one of four categories –
252 peripherals, module hubs, network hubs, and connectors – based on the within-module degree and
253 among-module connectivity (24, 55). Role analyses were only used the presence or absence of links
254 in the network and do not account for the link types (i.e. positive or negative associations).
255 To evaluate the effects of rootstocks on fungal diversity, Shannon entropy and species
256 richness were evaluated using the vegan package (64) wrapped by the phyloseq package (65) in R
257 (66). Differences in diversity across the rootstocks were compared using a mixed model ANOVA in
258 the lme4 package in R (67). Study site and sampling year were treated as random factors, blocked by
259 study sites, whereas the rootstock and compartments were treated as fixed factors. Changes in fungal
260 community composition across the samples were estimated based on a Bray-Curtis dissimilarity
261 distance matrix and visualized in non-metric multidimensional scaling (NMDS) plots. The
262 contribution of factors to the observed variation in fungal composition was estimated in a
263 permutational multivariate analysis of variance (PERMANOVA, using 1000 permutations) using the
264 adonis function in the vegan package (64). To identify OTUs that were sensitive to the rootstock
265 treatments, the observed frequency (proportion) of each OTU was evaluated by fitting a generalized
266 linear model (GLM) with negative binomial distribution, to identify depleted or enriched OTUs
267 (Differentially Abundant OTUs – DAOTUs). Likelihood ratio tests and contrast analyses (between
268 the hybrid rootstock and controls) were performed for the fitted GLM to identify the DAOTUs. We
269 used OTU frequencies from selfgrafts and nongrafts as controls, in comparisons with other
270 rootstocks, using contrasts. All tests were adjusted to control the false discovery rate (FDR, $p <$
271 0.01) using the Benjamini-Hochberg method (68). A differential abundance test was performed
272 within the controls (selfgraft vs. nongraft) to identify the OTUs responsive to the grafting
273 procedure, itself.

274 **RESULTS**

275 **RAF in the Grafted Tomato System**. Once rare OTUs (<10 sequence counts, which
276 accounted for more than 90% of the observed OTUs) were removed, the community consisted of
277 1586 OTUs and 1,063,017 sequences. Of these sequences, 4.8% remained unclassified at the phylum
278 level (Fig. S1). The classified sequences represented Ascomycota (52.5%), Basidiomycota (25.6%),
279 Zygomycota (11.5%), Chytridiomycota (3.6%), Glomeromycota (1.7%), and Rozellomycota (0.07%)
280 (Fig. 1). At the class level, Pezizomycetes, Agaricomycetes, and Dothideomycetes were the most
281 abundant across all the rootstocks. At the order level, the communities were dominated by Pezizales,
282 Pleosporales, Cantharellales, Mortierellales, and Hypocreales. Analyses at the family level revealed
283 that Pyronemataceae, Mortierellaceae, Ceratobasidiaceae, and Pleosporaceae were the most common
284 taxa overall. At the genus level, *Mortierella*, *Thanatephorus*, and *Alternaria* were the most abundant
285 genera.

286 **Effects of Grafting and Rootstock on α-Diversity.** There was strong evidence for a
287 rootstock effect on OTU richness ($F_{1, 3} = 8.6$, $p < 0.001$) and Shannon entropy ($F_{1, 3} = 3.2$, $p = 0.02$)
288 for tomato RAF communities. Mean species richness was higher in both the endosphere ($p = 0.01$)
289 and rhizosphere ($p = 0.001$) of one of the hybrid rootstocks, Maxifort, compared to the nongrafted
290 control. Shannon entropy followed trends similar to richness with a higher estimate for Maxifort;
291 however, there was only evidence for higher Shannon entropy in Maxifort for the rhizosphere ($p =$
292 0.004), but not for the endosphere ($p = 0.6$) (Fig. 2). Both species richness and Shannon entropy
293 were higher ($p < 0.001$) in the rhizosphere than in the endosphere across all the rootstock genotypes
294 (Fig. S2).

295 **Effects of Grafting and Rootstock on RAF Composition.** Based on previous studies of
296 the plant genotype effect on the rhizobiome (47), we expected a significant rootstock effect on
297 community composition. Rootstock explained 2% of the variation in the RAF community
298 composition (PERMANOVA; $p<0.01$), whereas compartment, study site, and year explained a
299 greater proportion of the variation than rootstock (Fig. S3 and Table S2). Endosphere-rhizosphere
300 compartments accounted for 8.92% of the variation. Study site and interannual variation explained
301 8.34% and 5.38% of the total variation, respectively (Table S2).

302 **Comparison of DAOTUs.** The analysis of differential abundance found effects of
303 rootstock genotype at the individual OTU level. While analyses of alpha diversity indicated higher
304 diversity in the rhizosphere than in the endosphere, we observed the opposite in the analysis of
305 DAOTUs, with nearly twice as many DAOTUs in the endosphere (n = 146 i.e. 9.2% of the total

306 OTUs) compared to the rhizosphere (n = 76 i.e. 4.8% of total OTUs) (Figs. 2 and S4). Comparison
307 across rootstocks indicated a greater number of DAOTUs in Maxifort (n = 80) than in RST-04-106
308 (n = 66) and the selfgraft control (n = 49). Compared to the hybrid rootstocks, the number of
309 depleted taxa was greater in the selfgraft control (n = 28). Among the enriched OTUs in Maxifort,
310 27 OTUs belonged to Basidiomycota, 20 to Ascomycota, and 11 to Glomeromycota, whereas four
311 basidiomycete, three ascomycete, and one zygomycete OTUs were depleted in Maxifort. In RST-04-
312 106, enriched taxa included 22 OTUs in Basidiomycota, 20 OTUs in Ascomycota and five OTUs in
313 Glomeromycota, whereas the depleted OTUs included six in Zygomycota. Comparing the self- and
314 nongraft controls, nine OTUs in Ascomycota, three OTUs in Basidiomycota, and four OTUs in
315 Zygomycota were enriched in the selfgraft treatment, whereas 12 OTUs in Basidiomycota, seven
316 OTUs in Ascomycota, four OTUs in Zygomycota, and three OTUs in Glomeromycota were
317 depleted in the selfgraft treatment.
318 **Network Analysis/ General Network Structures.** Fungal community complexity,
319 defined in terms of mean node degree and community structures/motifs, varied among the
320 rootstocks in both the endosphere and the rhizosphere, with a greater mean node degree in one of
321 the hybrid rootstocks, Maxifort, compared to both controls and RST-04-106 (Figs. 3, S5, S6, and
322 Table S3). Complexity was higher in the rhizosphere than in the endosphere compartment (Figs. 3,
323 S5, S6, and Table S3). In addition to the total number of links, the link type (either positive or
324 negative) differed among the rootstocks in both compartments (Table S3), with a higher ratio of
325 negative to positive links in Maxifort in both the endosphere and the rhizosphere compartments.
326 Rhizosphere fungal communities had a higher ratio of negative to positive links than those in the
327 endosphere, for all rootstocks. Although we observed rootstock-specific or compartment-specific
328 effects on the node degree and ratio of negative to positive links, the number of modules defined
329 using a simulated annealing (SA) algorithm were similar in both the endosphere and rhizosphere
330 compartments and across the rootstocks (Table S3). Our analyses of node types divided the
331 observed nodes in the association-network into four categories: peripherals, module hubs, network
332 hubs, and connectors. More taxa in the rhizosphere were identified as key nodes than in the
333 endosphere, and key nodes were more common in the hybrid rootstocks than in the non- and
334 selfgrafted controls (Figs. 4 and 5).
335 **Lasso regression, GLM, and PhONA.** Using lasso regression and GLM models, we
336 identified the OTUs predictive of tomato yield in each compartment in each rootstock. The number
337 of predictive OTUs identified by the varImp function was about the same across the rootstock

338 treatments in both the compartments. However, not all the predicted OTUs were associated with
339 other OTUs in the network models. The Maxifort rhizosphere had the highest number of OTUs
340 (10) associated with other OTUs in the network models. Only a subset of the entire microbiome was
341 predictive of the yield, among which only a few microbes were associated with other microbes in the
342 network models.

343 **DISCUSSION**

344 This study demonstrated the effect of rootstocks on RAF community composition and structure.
345 General diversity-based analyses indicated a rootstock effect. The most productive hybrid rootstock,
346 Maxifort, supported higher fungal richness and Shannon entropy, as well as a greater number of
347 DAOTUs than the controls, consistent with the expectation that higher diversity and a higher
348 number of responsive taxa (DAOTUs) would be associated with a more productive genotype. Also
349 consistent with our expectations, we observed higher microbial diversity and fewer responsive taxa
350 (DAOTUs) in the rhizosphere compared to the endosphere. The integrated host phenotype and
351 OTU network in the PhONA identified potential candidate taxa for each rootstock, and community
352 structures in the endosphere and rhizosphere compartments. The general network analysis found
353 more interactions and more complex network structures in fungal communities associated with
354 Maxifort, consistent with our expectation that a more productive rootstock would have greater
355 community complexity. Community complexity, when defined in terms of mean node degree,
356 differed between the root compartments: the endosphere community was less complex than the
357 rhizosphere community in all the rootstocks. Overall, our study i) showed that rootstocks and
358 grafting are significant drivers of RAF community composition, diversity and structure, and ii)
359 introduced and illustrated the use of PhONA as an analytical framework to select potential
360 candidates for microbiome-based agriculture. Potential candidates are those taxa that were directly
361 predictive of higher yield (taxa with direct positive links with the yield node in the network), taxa
362 that have positive associations with taxa positively associated with yield, and/or taxa that have
363 negative associations with taxa negatively associated with yield. There is the potential to consider
364 taxa multiple steps removed from the yield response, with the understanding that uncertainty about
365 the link to yield increases the more steps the taxon is from the yield node. From a practical
366 standpoint, our results indicate the potential for using plant genotypes and agricultural practices to
367 modulate plant-associated microbial communities, and the potential for the PhONA framework to
368 improve identification of candidate taxa to support microbiome-based crop production.

369 In contrast to network models that portray only microbe-microbe interactions, PhONA
370 integrates the results of GLM models of microbe association with phenotypic traits to support
371 inference about candidate taxa and predictive microbiome analyses. Thus, candidate taxa can be
372 selected not only because they have a direct association with the host response variable(s), but also
373 because they are indirectly associated with the host response variable through their associations with
374 community members that have direct associations with host traits. For instance, a node that has a
375 positive association with the system phenotype node (in our case, yield) might have negative or
376 positive associations with other OTUs. Such OTUs with indirect positive associations with the
377 desired phenotype might also be included in biofertilizer consortia. Using a PhONA, a rational
378 consortium can be selected based on the phenotype of interest. Applying PhONA for disease or
379 pathogen resistance phenotypes could be useful for designing rational biocontrol consortia. We also
380 observed some OTUs with direct negative associations with the yield node. Efforts to control
381 negatively associated taxa, as well as the taxa that have positive associations with these taxa, might
382 contribute to maximizing yield. Although we did not observe any disease symptoms in our
383 experiments, OTUs negatively associated with the yield node might represent a case of
384 asymptomatic negative microbial effects on yield. Efforts to explore negatively associated OTUs
385 might provide opportunities to minimize asymptomatic yield loss in crops.
386 The main goal of PhONA is to provide a systems framework to generate hypotheses about
387 the role of microbiome components in host function and performance, and to support the potential
388 for mechanistic/predictive models to better understand host-microbiome interactions. *In planta*
389 experiments with fungal cultures are essential to test the hypotheses generated by these models, to
390 help to differentiate between associations that are based on consistent biological interactions and not
391 simply based on shared (or opposing) environmental niche preferences. It is important to be
392 cautious in attributing biological interactions to the key structures in network attributes because the
393 links in the PhONA may or may not depict biological interactions. That is, many links may represent
394 only correlative relationships and not causal ones (28). For instance, the hub node in the network is
395 often regarded as a key node, but the high number of links with the hub node in the association
396 network could be due to shared niches, biological interactions, or a mixture thereof. If the
397 associations are mostly due to shared niches, removing such a hub node will have a more limited
398 effect, whereas removal of a hub node involved in many biological interactions could lead to
399 significant effects on the microbial community.

400 RAF community composition, diversity, and interactions differed between the endosphere
401 and rhizosphere compartments. Although the endosphere and the rhizosphere are physically
402 adjacent, they are distinct in community composition and diversity. Compartment specificity in
403 community composition and diversity has been reported for other plant species, in both natural and
404 agricultural settings (31, 69, 70). Usually, bulk soil is considered a source of microbial communities, a
405 subset of which is selected for in the rhizosphere (31, 71), mainly as a function of root exudates and
406 rhizodeposits (43, 72-75). Selection of the rhizosphere microbiome could be specific (*e.g.*,
407 antagonistic to plant pathogens) (76, 77) or more general with less influence of host genotype. In
408 comparison, the endosphere of host plants often supports lower microbial diversity compared to the
409 rhizosphere (70, 71). Host tissues and defense systems act as biotic filters (2). As a result, the
410 microbiome is more specialized in the endosphere than in the rhizosphere. RAF compartment
411 specificity may also be an important consideration for microbe-based disease management strategies
412 – especially for the management of pathogens or pests that are compartment specific, such as
413 endoparasites and ectoparasites.
414 RAF community composition and diversity also differed among the rootstock genotypes.
415 Plant genotypes can structure root-associated fungal communities (31, 70, 78). The commercial
416 rootstocks in our study have been bred to provide resistance against specific soilborne pathogens
417 and pests. Small host genotypic differences could alter the physiological and immunological
418 responses in the root systems, thereby selecting genotype-specific RAF communities (79). For
419 example, some root exudates and metabolites could be specific to a plant genotype (80-82) and
420 provide specific control of microbial communities (83-85). In some cases, the host genotype effect
421 can be directly attributed to root anatomy (77, 85, 86). Efficient root types and architectures are
422 desired agronomic traits to cope with biotic and abiotic stresses (87), and root systems vary among
423 and within plant species (86). Moreover, the effect of plant genotypes on microbial communities in
424 the root system may be linked to the flow of nutrients between the aboveground-scion and
425 belowground-rootstocks, where vigorous rootstock genotypes could drive greater resources to the
426 microbial communities by supporting larger scion biomass. In such a positive nutrient feedback
427 between the scion and rootstock, rootstock genotype appears to be a more critical driver than the
428 scion genotype (88). Rootstock genotypes supporting higher yield and biomass may support higher
429 microbial diversity by excreting a greater volume of photosynthates as root exudates and
430 metabolites. Although we did not evaluate root exudates, and used the same scion across the study,
431 our study is consistent with a role of higher yield and biomass (as for the Maxifort rootstock) being

432 associated with higher fungal diversity. Additionally, we observed an effect of rootstock on the RAF
433 community composition. Collectively, the results support our expectations of rootstock-specific
434 control of the RAF community.

435 Our definition of complexity is based on interactions in networks, using a definition similar
436 to that used in other microbiome network analyses (25, 34, 89). However, a greater number of
437 interactions and complex network structures/motifs would tend to be observed whenever more
438 nodes exist in these association networks, an inherent relationship not always considered in studies
439 of complexity in microbiomes. The higher number of OTUs associated with Maxifort would tend
440 to result in higher complexity compared to rootstocks with fewer OTUs. Another potential measure
441 of complexity is network density, the proportion of links observed in a network relative to the total
442 number of possible links. For all the rootstocks we studied, network density was similar (0.04) in
443 both compartments, indicating similar community complexity. Statistical methods comparable to
444 rarefaction, designed to equalize the number of nodes across networks or methods to balance OTU
445 richness for sampling efforts (90), will be a valuable future effort for understanding how network
446 complexity responds to treatments and for making comparisons across studies. In addition, methods
447 to optimize and automate the selection of association thresholds to define the pairwise relationships
448 in a microbiome network is a gap and opportunity for improving microbiome network analyses. For
449 graphics in the figures in this analysis, we selected a level of association such that an interpretable
450 number of OTUs were depicted for visual consideration. Studies directly applied to identify
451 potential microbial assemblages for agricultural applications could benefit from exploring results for
452 a range of thresholds.

453 Our study indicates the rootstock-genotype specific effect on RAF diversity, composition,
454 and interactions, and also demonstrates integration of system phenotypes such as plant yield in a
455 network-based model to support selection of candidate taxa for biological use. However, in
456 sequence-based studies such as ours, the biological and functional significance of the candidate
457 OTUs remains unknown. Follow-up experiments with fungal cultures will be necessary to determine
458 the biological roles of the candidate OTUs, and to differentiate causal associations from correlations
459 based on niche preference. Similarly, further development of PhONA to incorporate temporal
460 microbiome data and Bayesian learning and inference methodologies (91, 92) has the potential to
461 support causal inference, including understanding of directionality in microbiome networks.
462 PhONA utilizes a lasso regression and GLM to link OTUs with a system phenotype, although many
463 other models such as random forest and other machine learning approaches (93) could also be

464 employed. Given the nature of microbiome data, having a high number of features (p) and relatively
465 small number of samples (n), other models to address the n x p problem can improve PhONA
466 predictions. Rather than pure prediction, our methods aim to find the key predictors and use them
467 in the GLM model for evaluating associations with the yield response. PhONA focused on finding
468 the attributable predictors/OTUs that are key to biological interventions, which are missed in
469 approaches that are focused purely on prediction (94). Smaller sample size was a limitation in our
470 current study, reflecting the challenge of processing a large number of plant replicates, and we did
471 not validate the results from our model by splitting data into training and test sets. A rigorous model
472 validation step would improve the accuracy of PhONA. As lab-based technologies and
473 computational resources become less expensive, studies with large sample sizes are becoming more
474 practical and, when combined with an analytical framework like PhONA, microbial community
475 analyses can go beyond simple analyses of diversity to help make microbiome-based agriculture a
476 reality.
477

478 **Acknowledgements**

479 We appreciate support from the Ceres Trust, USDA NCR SARE Research and Education Grant
480 LNC13-355, Foundation for Food and Agriculture Research Grant
481 FF-NIA19-0000000050, the Kansas Agricultural Experiment Station, the National Institute for
482 Mathematical and Biological Synthesis (NIMBioS), and the University of Florida. We thank
483 members of the Garrett lab for their comments on an early version of the manuscript. R.P., K.A.G.,
484 A.J., M.M.K., and C.L.R. designed the study. R.P. and L.G.M. collected and processed the samples.
485 R.P. analyzed and interpreted the data. R.P., K.A.G., and A.J. wrote the manuscript. R.P., K.A.G.,
486 A.J., M.M.K., C.L.R., and L.G.M. revised the manuscript. All authors read and approved the final
487 manuscript.

488 **FIG 1** The Phenotype-OTU network analysis (PhONA) combines (A) an OTU-OTU association
489 network with (B) the nodes selected based on predictive model for their association with a host
490 phenotype variable such as yield, to create (C) a PhONA.
491
492 **FIG 2** Enriched and depleted OTUs across tomato rootstock genotype combinations (nongraft
493 BHN589, selfgraft BHN589, and BHN589 grafted on two hybrid rootstocks (RST-04-106 and
494 Maxifort)) evaluated for the rhizosphere (A) and the endosphere (B), using OTU counts from
495 selfgrafts and nongrafts as controls. All the tests were adjusted to control the false discovery rate
496 (FDR, $p < 0.01$) using the Benjamini-Hochberg method. Each point represents an OTU labeled at
497 the genus level and colored based on phylum, and the position along the x-axis represents the
498 abundance fold-change contrast with controls (except for the selfgraft vs. nongraft comparison,
499 where the nongraft treatment was used as a control for the contrast).
500
501 **FIG 3** Phenotype-OTU network analysis (PhONA) of endosphere fungal taxa for BHN589 grafted
502 on Maxifort. Node color indicates the phylum, except that the yellow-color node represents yield
503 associated with the rootstock. Nodes connected to the rootstock yield node with black links are taxa
504 that were predictive of rootstock yield, where dotted and solid lines indicate negative and positive
505 associations with the yield node, respectively. Red and blue links represent negative and positive
506 associations, respectively, between OTUs. Nodes are labeled with the finest-resolution taxonomic
507 categorization available.
508
509 **FIG 4** Partitioning of endosphere fungal OTUs according to their network roles. Nodes were
510 divided into four categories based on within-module degree and among-module connectivity. The
511 blue dashed line represents a threshold value (0.62) for among-module connectivity, and the red
512 dashed line represents a threshold value (2.5) for within-module degree. Nodes were categorized as
513 peripherals, connectors, module hubs, and network hubs. Node color indicates rootstock treatment
514 (nongraft BHN589, selfgraft BHN589, and BHN589 grafted on two hybrid rootstocks (RST-04-106
515 and Maxifort)).
516
517 **FIG 5** Partitioning of rhizosphere fungal OTUs according to their network roles. Nodes were
518 divided into four categories based on within-module degree and among-module connectivity. The
519 blue dashed line represents a threshold value (0.62) for among-module connectivity, and the red
520 dashed line represents a threshold value (2.5) for within-module degree. Nodes were categorized as
521 peripherals, connectors, module hubs, and network hubs. Node color indicates rootstock treatment
522 (nongraft BHN589, selfgraft BHN589, and BHN589 grafted on two hybrid rootstocks (RST-04-106
523 and Maxifort)).
524
525 **FIG S1** Relative abundance of endosphere and rhizosphere fungi at the phylum level recovered
526 from four tomato rootstock treatments: nongraft BHN589, selfgraft BHN589, and BHN589 grafted
527 on two hybrid rootstocks (RST-04-106 and Maxifort). Each individual bar represents a rootstock
528 treatment, and the colored area within the bar represents the relative abundance of the
529 corresponding phylum.
530
531 **FIG S2** Comparison of overall fungal diversity (A) and richness (B) associated with tomato
532 rootstock genotypes and controls, evaluated in the endosphere and rhizosphere. The plot is divided
533 by the four tomato rootstock treatments: nongraft BHN589, selfgraft BHN589, and BHN589
534 grafted on two hybrid rootstocks (RST-04-106 and Maxifort). Shannon entropy and species richness,
535 measures of community diversity, were both higher for Maxifort ($p < 0.005$) compared to the self-

graft and RST-04-106 in the rhizosphere, while there was not evidence for a difference in Shannon entropy in the endosphere ($p = 0.634$). Treatment means were separated using the "difflsmeans" function as specified in the lmerTest package in R. Tests for boxplots sharing a letter or letter case type had $p > 0.05$.

FIG S3 Non-metric multidimensional scaling (NMDS) ordination plot of samples labeled by tomato rootstock (nongraft BHN589, selfgraft BHN589, and BHN589 grafted on two hybrid rootstocks (RST-04-106 and Maxifort)), compartment (endosphere or rhizosphere), and study site, based on the Bray-Curtis dissimilarity distance matrix of fungal OTUs. Color indicates rootstock treatment, shape indicates study site, and size indicates compartment. Ellipses surrounding the samples indicate the 95% CI of the endosphere and rhizosphere sample centroids.

FIG S4 Number of DAOTUs in a contrast analysis, evaluated for the endosphere and rhizosphere compartments for four tomato rootstock treatments: nongraft and selfgraft BHN589, and BHN589 grafted on two hybrid rootstocks (Maxifort and RST-04-106). The green color in each bar represents the number of enriched taxa, and the red color represents the number of depleted taxa. The number of differentially changed taxa was greater for the endosphere than for the rhizosphere. Among the contrast pairs, hybrid rootstocks had a greater number of enriched taxa compared to depleted taxa. However, the number of depleted taxa was higher compared to enriched taxa in the controls. Among the treatments, Maxifort had the highest number of DAOTUs in both compartments.

FIG S5 Phenotype-OTU network analysis (PhONA) of endosphere fungal taxa for tomato rootstock treatments: (A) nongraft and (B) selfgraft BHN589, and (C) BHN589 grafted on RST-04-106. Node color indicates the phylum, except that the yellow-color node represents yield associated with the rootstock. Nodes connected to the rootstock yield node with black links are taxa that were predictive of rootstock yield, where dotted and solid lines indicate negative and positive associations with the yield node, respectively. Red and blue links represent negative and positive associations, respectively, between OTUs. Nodes are labeled with the finest-resolution taxonomic categorization available.

FIG S6 Phenotype-OTU network analysis (PhONA) of rhizosphere fungal taxa for tomato rootstock treatments: (A) nongraft and (B) selfgraft BHN589, and BHN589 grafted on two hybrid rootstocks ((C) RST-04-106 and (D) Maxifort). Node color indicates the phylum, except that the tomato-color node represents yield associated with the rootstock. Nodes connected to the rootstock yield node with black links are taxa that were predictive of rootstock yield, where dotted and solid lines indicate negative and positive associations with the yield node, respectively. Red and blue links represent negative and positive associations, respectively, between OTUs. Nodes are labeled with the finest-resolution taxonomic categorization available.

TABLE S1 Sites included in the study, their soil type, and geographic coordinates.

TABLE S2 Results of the multivariate permutational analysis of variance (PERMANOVA) for fungal taxon abundance data. Permutation was based on the Bray-Curtis distance matrix generated for root associated fungal communities at the OTU level from four tomato rootstock treatments: nongraft and selfgraft BHN589, and BHN589 grafted on two hybrid rootstocks (Maxifort and RST-04-106) (1000 permutations). P values < 0.05 are in bold.

583 **TABLE S3** Network attributes and links observed in the fungal association networks for four
584 tomato rootstock treatments: nongraft and selfgraft BHN589, and BHN589 grafted on two hybrid
585 rootstocks (Maxifort and RST-04-106) in each of rhizosphere and endosphere compartments.
586
587 REFERENCES
588

589 1. Berendsen RL, Pieterse CM, Bakker PA. 2012. The rhizosphere microbiome and plant
590 health. Trends Plant Sci 17:478-86.
591 2. Lebeis SL, Paredes SH, Lundberg DS, Breakfield N, Gehring J, McDonald M, Malfatti S,
592 del Rio TG, Jones CD, Tringe SG, Dangl JL. 2015. Salicylic acid modulates colonization
593 of the root microbiome by specific bacterial taxa. Science 349:860-864.
594 3. Panke-Buisse K, Poole AC, Goodrich JK, Ley RE, Kao-Kniffin J. 2015. Selection on soil
595 microbiomes reveals reproducible impacts on plant function. ISME J 9:980-9.
596 4. Turnbaugh PJ, Hamady M, Yatsunenko T, Cantarel BL, Duncan A, Ley RE, Sogin ML,
597 Jones WJ, Roe BA, Affourtit JP, Egholm M, Henrissat B, Heath AC, Knight R, Gordon
598 JI. 2009. A core gut microbiome in obese and lean twins. Nature 457:480-4.
599 5. Xue C, Penton CR, Shen Z, Zhang R, Huang Q, Li R, Ruan Y, Shen Q. 2015.
600 Manipulating the banana rhizosphere microbiome for biological control of Panama
601 disease. Sci Rep 5:11124.
602 6. Gould AL, Zhang VV, Lamberti L, Jones EW, Obadia B, Korasidis N, Gavryushkin A,
603 Carlson JM, Beerenwinkel N, Ludington WB. 2018. Microbiome interactions shape host
604 fitness. Proc Natl Acad Sci USA 115:E11951-E11960.
605 7. Zhou X, Wang JT, Wang WH, Tsui CK, Cai L. 2020. Changes in bacterial and fungal
606 microbiomes associated with tomatoes of healthy and infected by *Fusarium oxysporum f.*
607 *sp. lycopersici*. Microb Ecol doi:10.1007/s00248-020-01535-4.
608 8. Kaur S, Egidi E, Qiu Z, Macdonald CA, Verma JP, Trivedi P, Wang J, Liu H, Singh BK.
609 2022. Synthetic community improves crop performance and alters rhizosphere microbial
610 communities. J Sustain Agric 1:118-131.
611 9. Jin CW, Ye YQ, Zheng SJ. 2014. An underground tale: Contribution of microbial activity
612 to plant iron acquisition via ecological processes. Ann Bot 113:7-18.
613 10. Koide RT. 1991. Nutrient supply, nutrient demand and plant-response to mycorrhizal
614 infection. New Phytol 117:365-386.
615 11. Mishra PK, Bisht SC, Mishra S, Selvakumar G, Bisht JK, Gupta HS. 2012. Coinoculation
616 of *rhizobium leguminosarum*-pr1 with a cold tolerant *pseudomonas* sp. Improves iron
617 acquisition, nutrient uptake and growth of field pea (*pisum sativum l.*). J Plant Nutr
618 35:243-256.
619 12. Mendes R, Kruijt M, de Bruijn I, Dekkers E, van der Voort M, Schneider JHM, Piceno
620 YM, DeSantis TZ, Andersen GL, Bakker PAHM, Raaijmakers JM. 2011. Deciphering
621 the rhizosphere microbiome for disease-suppressive bacteria. Science 332:1097-1100.
622 13. Gaiero JR, McCall CA, Thompson KA, Day NJ, Best AS, Dunfield KE. 2013. Inside the
623 root microbiome: Bacterial root endophytes and plant growth promotion. Am J Bot
624 100:1738-50.
625 14. Glick BR. 1995. The enhancement of plant-growth by free-living bacteria. Can J
626 Microbiol 41:109-117.
627 15. Conrath U. 2009. Priming of induced plant defense responses. Plant Innate Immunity
628 51:361-395.

629 16. Pieterse CMJ, Zamioudis C, Berendsen RL, Weller DM, Van Wees SCM, Bakker
630 PAHM. 2014. Induced systemic resistance by beneficial microbes. Annu Rev
631 Phytopathol 52:347-375.
632 17. Marasco R, Rolli E, Ettoumi B, Vigani G, Mapelli F, Borin S, Abou-Hadid AF, El-
633 Behairy UA, Sorlini C, Cherif A, Zocchi G, Daffonchio D. 2012. A drought resistance-
634 promoting microbiome is selected by root system under desert farming. PLoS One 7(10):
635 e48479.
636 18. Yang J, Kloepper JW, Ryu CM. 2009. Rhizosphere bacteria help plants tolerate abiotic
637 stress. Trends Plant Sci 14:1-4.
638 19. Yuan ZL, Druzhinina IS, Labbe J, Redman R, Qin Y, Rodriguez R, Zhang CL, Tuskan
639 GA, Lin FC. 2016. Specialized microbiome of a halophyte and its role in helping non-
640 host plants to withstand salinity. Sci Rep 6:32467.
641 20. Mazzola M, Freilich S. 2017. Prospects for biological soilborne disease control:
642 Application of indigenous versus synthetic microbiomes. Phytopathology 107:256-263.
643 21. Xu XM, Jeffries P, Pautasso M, Jeger MJ. 2011. Combined use of biocontrol agents to
644 manage plant diseases in theory and practice. Phytopathology 101:1024-1031.
645 22. Shayanthan A, Ordoñez PAC, Oresnik IJ. 2022. The role of synthetic microbial
646 communities (syncom) in sustainable agriculture. Frontiers in Agronomy 4.
647 23. de Souza RSC, Armanhi JSL, Arruda P. 2020. From microbiome to traits: Designing
648 synthetic microbial communities for improved crop resiliency. Front Plant Sci 11:1179.
649 24. Agler MT, Ruhe J, Kroll S, Morhenn C, Kim ST, Weigel D, Kemen EM. 2016. Microbial
650 hub taxa link host and abiotic factors to plant microbiome variation. PLoS Biol 14(1):
651 e1002352.
652 25. Shi S, Nuccio EE, Shi ZJ, He Z, Zhou J, Firestone MK. 2016. The interconnected
653 rhizosphere: High network complexity dominates rhizosphere assemblages. Ecol Lett
654 19:926-36.
655 26. Ascunce MS, Shin K, Huguet-Tapia JC, Poudel R, Garrett KA, van Bruggen AHC, Goss
656 EM. 2018. Penicillin trunk injection affects bacterial community structure in citrus trees.
657 Microb Ecol 78:457–469.
658 27. Garrett KA, Alcala-Briseno RI, Andersen KF, Buddenhagen CE, Choudhury RA, Fulton
659 JC, Hernandez Nopsa JF, Poudel R, Xing Y. 2018. Network analysis: A systems
660 framework to address grand challenges in plant pathology. Annu Rev Phytopathol
661 56:559-580.
662 28. Poudel R, Jumpponen A, Schlatter DC, Paulitz TC, Gardener BBM, Kinkel LL, Garrett
663 KA. 2016. Microbiome networks: A systems framework for identifying candidate
664 microbial assemblages for disease management. Phytopathology 106:1083-1096.
665 29. Rottjers L, Faust K. 2018. From hairballs to hypotheses-biological insights from
666 microbial networks. Fems Microbiology Reviews 42:761-780.
667 30. Wang Z, Bafadhel M, Haldar K, Spivak A, Mayhew D, Miller BE, Tal-Singer R,
668 Johnston SL, Ramsheh MY, Barer MR, Brightling CE, Brown JR. 2016. Lung
669 microbiome dynamics in copd exacerbations. European Respiratory Journal 47:1082-
670 1092.
671 31. Cregger MA, Veach AM, Yang ZK, Crouch MJ, Vilgalys R, Tuskan GA, Schadt CW.
672 2018. The *Populus* holobiont: Dissecting the effects of plant niches and genotype on the
673 microbiome. Microbiome 6:31.

674 32. Edwards JA, Santos-Medellin CM, Liechty ZS, Nguyen B, Lurie E, Eason S, Phillips G,
675 Sundaresan V. 2018. Compositional shifts in root-associated bacterial and archaeal
676 microbiota track the plant life cycle in field-grown rice. PLoS Biol 16:e2003862.
677 33. Fitzpatrick CR, Copeland J, Wang PW, Guttman DS, Kotanen PM, Johnson MTJ. 2018.
678 Assembly and ecological function of the root microbiome across angiosperm plant
679 species. Proc Natl Acad Sci USA 115:E1157-E1165.
680 34. Marasco R, Rolli E, Fusi M, Michoud G, Daffonchio D. 2018. Grapevine rootstocks
681 shape underground bacterial microbiome and networking but not potential functionality.
682 Microbiome 6:3.
683 35. Wagner MR, Lundberg DS, del Rio TG, Tringe SG, Dangl JL, Mitchell-Olds T. 2016.
684 Host genotype and age shape the leaf and root microbiomes of a wild perennial plant. Nat
685 Commun 7:12151.
686 36. Herrera J, Poudel R, Bokati D. 2013. Assessment of root-associated fungal communities
687 colonizing two species of tropical grasses reveals incongruence to fungal communities of
688 North American native grasses. Fungal Ecol 6:65-69.
689 37. French E, Tran T, Iyer-Pascuzzi AS. 2020. Tomato genotype modulates selection and
690 responses to root microbiota. Phytobiomes Journal doi:10.1094/pbiomes-02-20-0020-r.
691 38. Bulgarelli D, Schlaeppi K, Spaepen S, Ver Loren van Themaat E, Schulze-Lefert P.
692 2013. Structure and functions of the bacterial microbiota of plants. Annu Rev Plant Biol
693 64:807-38.
694 39. Hol WHG, Bezemer TM, Biere A. 2013. Getting the ecology into interactions between
695 plants and the plant growth-promoting bacterium *Pseudomonas fluorescens*. Front Plant
696 Sci 4:81.
697 40. Ortiz-Castro R, Contreras-Cornejo HA, Macias-Rodriguez L, Lopez-Bucio J. 2009. The
698 role of microbial signals in plant growth and development. Plant Signal Behav 4:701-12.
699 41. Edwards J, Johnson C, Santos-Medellín C, Lurie E, Podishetty NK, Bhatnagar S, Eisen
700 JA, Sundaresan V. 2015. Structure, variation, and assembly of the root-associated
701 microbiomes of rice. Proc Natl Acad Sci USA 112:E911-E920.
702 42. Lundberg DS, Lebeis SL, Paredes SH, Yourstone S, Gehring J, Malfatti S, Tremblay J,
703 Engelbrektson A, Kunin V, del Rio TG, Edgar RC, Eickhorst T, Ley RE, Hugenholtz P,
704 Tringe SG, Dangl JL. 2012. Defining the core *Arabidopsis thaliana* root microbiome.
705 Nature 488:86-90.
706 43. Wang P, Marsh EL, Ainsworth EA, Leakey ADB, Sheflin AM, Schachtman DP. 2017.
707 Shifts in microbial communities in soil, rhizosphere and roots of two major crop systems
708 under elevated CO2 and O3. Sci Rep 7:15019.
709 44. Herrera J, Poudel R, Nebel KA, Collins SL. 2011. Precipitation increases the abundance
710 of some groups of root-associated fungal endophytes in a semiarid grassland. Ecosphere
711 2(4):art50.
712 45. Bokati D, Herrera J, Poudel R. 2016. Soil influences colonization of root-associated
713 fungal endophyte communities of maize, wheat, and their progenitors. J Mycol 2016:1-9.
714 46. Meyer L. 2016. Grafting to increase high tunnel tomato productivity in the central united
715 states. Master Thesis. http://hdl.handle.net/2097/32736.
716 47. Poudel R, Jumpponen A, Kennelly MM, Rivard CL, Gomez-Montano L, Garrett KA.
717 2019. Rootstocks shape the rhizobiome: Rhizosphere and endosphere bacterial
718 communities in the grafted tomato system. Appl Environ Microbiol 85:01765–01718.

48. Tibshirani R. 1996. Regression shrinkage and selection via the lasso. Journal of the Royal Statistical Society Series B (Methodological) 58:267-288.
49. Roguet A, Eren AM, Newton RJ, McLellan SL. 2018. Fecal source identification using random forest. Microbiome 6:185.
50. Belk A, Xu ZZ, Carter DO, Lynne A, Bucheli S, Knight R, Metcalf JL. 2018. Microbiome data accurately predicts the postmortem interval using random forest regression models. Genes 9(2):104.
51. Niu B, Paulson JN, Zheng XQ, Kolter R. 2017. Simplified and representative bacterial community of maize roots. Proc Natl Acad Sci USA 114:E2450-E2459.
52. Paredes SH, Gao TX, Law TF, Finkel OM, Mucyn T, Teixeira PJPL, Gonzalez IS, Feltcher ME, Powers MJ, Shank EA, Jones CD, Jojic V, Dangl JL, Castrillo G. 2018. Design of synthetic bacterial communities for predictable plant phenotypes. Plos Biology 16.
53. Kurtz ZD, Muller CL, Miraldi ER, Littman DR, Blaser MJ, Bonneau RA. 2015. Sparse and compositionally robust inference of microbial ecological networks. PLoS Comp Biol 11.
54. Friedman J, Alm EJ. 2012. Inferring correlation networks from genomic survey data. PLoS Comput Biol 8:e1002687.
55. Tackmann J, Matias Rodrigues JF, von Mering C. 2019. Rapid inference of direct interactions in large-scale ecological networks from heterogeneous microbial sequencing data. Cell Syst 9:286-296 e8.
56. Faust K, Raes J. 2016. Conet app: Inference of biological association networks using cytoscape. F1000Res 5:1519.
57. Gardes M, Bruns TD. 1993. Its primers with enhanced specificity for basidiomycetes--application to the identification of mycorrhizae and rusts. Mol Ecol 2:113-8.
58. Ihrmark K, Bodeker ITM, Cruz-Martinez K, Friberg H, Kubartova A, Schenck J, Strid Y, Stenlid J, Brandstrom-Durling M, Clemmensen KE, Lindahl BD. 2012. New primers to amplify the fungal ITS2 region - evaluation by 454-sequencing of artificial and natural communities. FEMS Microbiol Ecol 82:666-677.
59. Schloss PD, Westcott SL, Ryabin T, Hall JR, Hartmann M, Hollister EB, Lesniewski RA, Oakley BB, Parks DH, Robinson CJ, Sahl JW, Stres B, Thallinger GG, Van Horn DJ, Weber CF. 2009. Introducing mothur: Open-source, platform-independent, community-supported software for describing and comparing microbial communities. Appl Environ Microbiol 75:7537-41.
60. Wang Q, Garrity GM, Tiedje JM, Cole JR. 2007. Naive bayesian classifier for rapid assignment of rRNA sequences into the new bacterial taxonomy. Appl Environ Microbiol 73:5261-7.
61. Koljalg U, Nilsson RH, Abarenkov K, Tedersoo L, Taylor AFS, Bahram M, Bates ST, Bruns TD, Bengtsson-Palme J, Callaghan TM, Douglas B, Drenkhan T, Eberhardt U, Duenas M, Grebenc T, Griffith GW, Hartmann M, Kirk PM, Kohout P, Larsson E, Lindahl BD, Luecking R, Martin MP, Matheny PB, Nguyen NH, Niskanen T, Oja J, Peay KG, Peintner U, Peterson M, Poldmaa K, Saag L, Saar I, Schuessler A, Scott JA, Senes C, Smith ME, Suija A, Taylor DL, Telleria MT, Weiss M, Larsson KH. 2013. Towards a unified paradigm for sequence-based identification of fungi. Mol Ecol 22:5271-5277.
62. Friedman J, Alm EJ. 2012. Inferring correlation networks from genomic survey data. PLoS Comput Biol 8:e1002687.

63. Kuhn M. 2008. Building predictive models in r using the caret package. Journal of Statistical Software 28.
64. Oksanen J, Blanchet F, Friendly M, Kindt R, Legendre P, McGlinn D, Minchin P, O'Hara R, Simpson G, Solymos P, Stevens M, Szoecs E, Wagner H. 2018. Vegan: Community ecology package. R package version 2.4-6.:39pp.
65. McMurdie PJ, Holmes S. 2013. Phyloseq: An r package for reproducible interactive analysis and graphics of microbiome census data. PLoS One 8(4): e61217.
66. R Core Team. 2021. R: A language and environment for statistical computing. R foundation for statistical computing, vienna, austria. Url https://www.R-project.Org.
67. Bates D, Machler M, Bolker BM, Walker SC. 2015. Fitting linear mixed-effects models using lme4. J Stat Softw 67:1-48.
68. Ferreira JA. 2007. The benjamini-hochberg method in the case of discrete test statistics. Int J Biostat 3:Article 11.
69. Coleman-Derr D, Desgarennes D, Fonseca-Garcia C, Gross S, Clingenpeel S, Woyke T, North G, Visel A, Partida-Martinez LP, Tringe SG. 2016. Plant compartment and biogeography affect microbiome composition in cultivated and native Agave species. New Phytol 209:798-811.
70. Poli A, Lazzari A, Prigione V, Voyron S, Spadaro D, Varese GC. 2016. Influence of plant genotype on the cultivable fungi associated to tomato rhizosphere and roots in different soils. Fungal Biol 120:862-872.
71. Gottel NR, Castro HF, Kerley M, Yang ZM, Pelletier DA, Podar M, Karpinets T, Uberbacher E, Tuskan GA, Vilgalys R, Doktycz MJ, Schadt CW. 2011. Distinct microbial communities within the endosphere and rhizosphere of *Populus deltoides* roots across contrasting soil types. Appl Environ Microbiol 77:5934-5944.
72. Badri DV, Vivanco JM. 2009. Regulation and function of root exudates. Plant Cell Environ 32:666-681.
73. Dennis PG, Miller AJ, Hirsch PR. 2010. Are root exudates more important than other sources of rhizodeposits in structuring rhizosphere bacterial communities? FEMS Microbiol Ecol 72:313-27.
74. van der Heijden MG, Schlaeppi K. 2015. Root surface as a frontier for plant microbiome research. Proc Natl Acad Sci USA 112:2299-300.
75. Seitz VA, McGivern BB, Daly RA, Chaparro JM, Borton MA, Sheflin AM, Kresovich S, Shields L, Schipanski ME, Wrighton KC, Prenni JE. 2022. Variation in root exudate composition influences soil microbiome membership and function. Appl Environ Microbiol 88:e0022622.
76. Berg G, Opelt K, Zachow C, Lottmann J, Gotz M, Costa R, Smalla K. 2006. The rhizosphere effect on bacteria antagonistic towards the pathogenic fungus Verticillium differs depending on plant species and site. FEMS Microbiol Ecol 56:250-261.
77. Tian T, Reverdy A, She Q, Sun B, Chai Y. 2020. The role of rhizodeposits in shaping rhizomicrobiome.
78. Reazin C, Baird R, Clark S, Jumpponen A. 2019. Chestnuts bred for blight resistance depart nursery with distinct fungal rhizobiomes. Mycorrhiza 29:313-324.
79. Cardarelli M, Rouphael Y, Kyriacou MC, Colla G, Pane C. 2020. Augmenting the sustainability of vegetable cropping systems by configuring rootstock-dependent rhizomicrobiomes that support plant protection.

80. Nasholm T, Huss-Danell K, Hogberg P. 2000. Uptake of organic nitrogen in the field by four agriculturally important plant species. Ecology 81:1155-1161.
81. Reeve JR, Smith JL, Carpenter-Boggs L, Reganold JP. 2008. Soil-based cycling and differential uptake of amino acids by three species of strawberry (Fragaria spp.) plants. Soil Biol Biochem 40:2547-2552.
82. U'Ren N. 2007. Types, amounts, and possible functions of compounds released into the rhizosphere by soil-grown plants, p 1-21, The rhizosphere doi:10.1201/9781420005585.ch1. CRC Press.
83. Beattie GA. 2018. Metabolic coupling on roots. Nat Microbiol 3:396-397.
84. Zhalnina K, Louie KB, Hao Z, Mansoori N, da Rocha UN, Shi SJ, Cho HJ, Karaoz U, Loque D, Bowen BP, Firestone MK, Northen TR, Brodie EL. 2018. Dynamic root exudate chemistry and microbial substrate preferences drive patterns in rhizosphere microbial community assembly. Nat Microbiol 3:470-480.
85. Iannucci A, Canfora L, Nigro F, De Vita P, Beleggia R. 2021. Relationships between root morphology, root exudate compounds and rhizosphere microbial community in durum wheat. Applied Soil Ecology doi:10.1016/j.apsoil.2020.103781.
86. Warschefsky EJ, Klein LL, Frank MH, Chitwood DH, Londo JP, von Wettberg EJB, Miller AJ. 2016. Rootstocks: Diversity, domestication, and impacts on shoot phenotypes. Trends Plant Sci 21:418-437.
87. Malamy JE. 2005. Intrinsic and environmental response pathways that regulate root system architecture. Plant Cell Environ 28:67-77.
88. Song F, Bai F, Wang J, Wu L, Jiang Y, Pan Z. 2020. Influence of citrus scion/rootstock genotypes on arbuscular mycorrhizal community composition under controlled environment condition. Plants 9:1-16.
89. Cao X, Zhao D, Xu H, Huang R, Zeng J, Yu Z. 2018. Heterogeneity of interactions of microbial communities in regions of taihu lake with different nutrient loadings: A network analysis. Sci Rep 8:8890.
90. Carlson CJ, Zipfel CM, Garnier R, Bansal S. 2019. Global estimates of mammalian viral diversity accounting for host sharing. Nat Ecol Evol 3:1070-1075.
91. McGeachie MJ, Sordillo JE, Gibson T, Weinstock GM, Liu YY, Gold DR, Weiss ST, Litonjua A. 2016. Longitudinal prediction of the infant gut microbiome with dynamic bayesian networks. Sci Rep 6:20359.
92. Penalver Bernabe B, Cralle L, Gilbert JA. 2018. Systems biology of the human microbiome. Curr Opin Biotechnol 51:146-153.
93. Topcuoglu BD, Lesniak NA, Ruffin MTt, Wiens J, Schloss PD. 2020. A framework for effective application of machine learning to microbiome-based classification problems. mBio 11.
94. Efron B. 2020. Prediction, estimation, and attribution. Journal of the American Statistical Association 115:636-655.

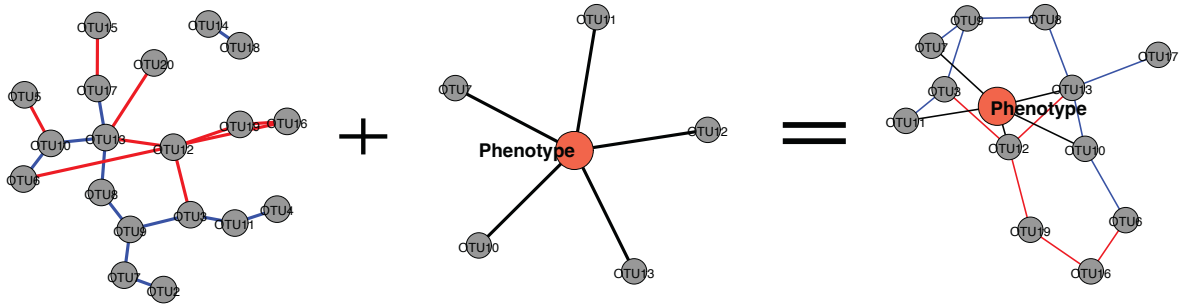

(A) OTU-OTU association network based on SparCC

(B) OTUs predictive of host phenotype, based on predictive model

(C) PhONA predicting candidate taxa based on association network **(A)** and phenotype-predictive OTUs **(B)**

FIG 1 The Phenotype-OTU network analysis (PhONA) combines (A) an OTU-OTU association network with (B) the nodes selected based on predictive model for their association with a host phenotype variable such as yield, to create (C) a PhONA.

853 (A)

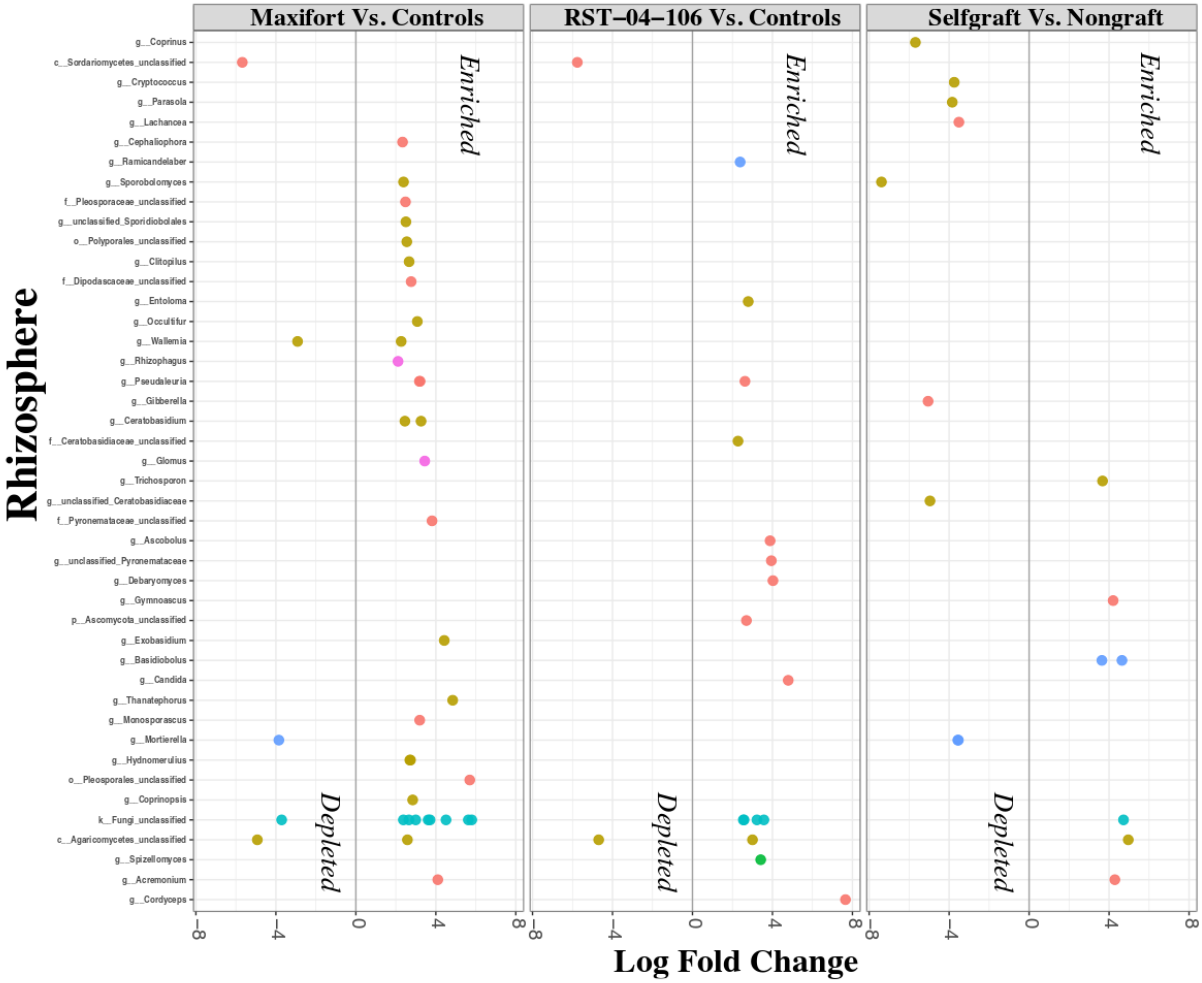
Selfgraft Vs. Nongraft
RST−04−106 Vs. Controls
Maxifort Vs. Controls
Enriched
Depleted
Log Fold Change
−8
−4
0
4
8
Rhizosphere
g__Coprinus
c__Sordariomycetes_unclassified
g__Cryptococcus
g__Parasola
g__Lachancea
g__Cephaliophora
g__Ramicandelaber
g__Sporobolomyces
f__Pleosporaceae_unclassified
g__unclassified_Sporidiobolales
o__Polyporales_unclassified
g__Clitopilus
f__Dipodascaceae_unclassified
g__Entoloma
g__Occultifur
g__Wallemia
g__Rhizophagus
g__Pseudaleuria
g__Gibberella
g__Ceratobasidium
f__Ceratobasidiaceae_unclassified
g__Glomus
g__Trichosporon
g__unclassified_Ceratobasidiaceae
f__Pyronemataceae_unclassified
g__Ascobolus
g__unclassified_Pyronemataceae
g__Debaryomyces
g__Gymnoascus
p__Ascomycota_unclassified
g__Exobasidium
g__Basidiobolus
g__Candida
g__Thanatephorus
g__Monosporascus
g__Mortierella
g__Hydnomerulius
o__Pleosporales_unclassified
g__Coprinopsis
k__Fungi_unclassified
c__Agaricomycetes_unclassified
g__Spizellomyces
g__Acremonium
g__Cordyceps

854
855

856 (B)

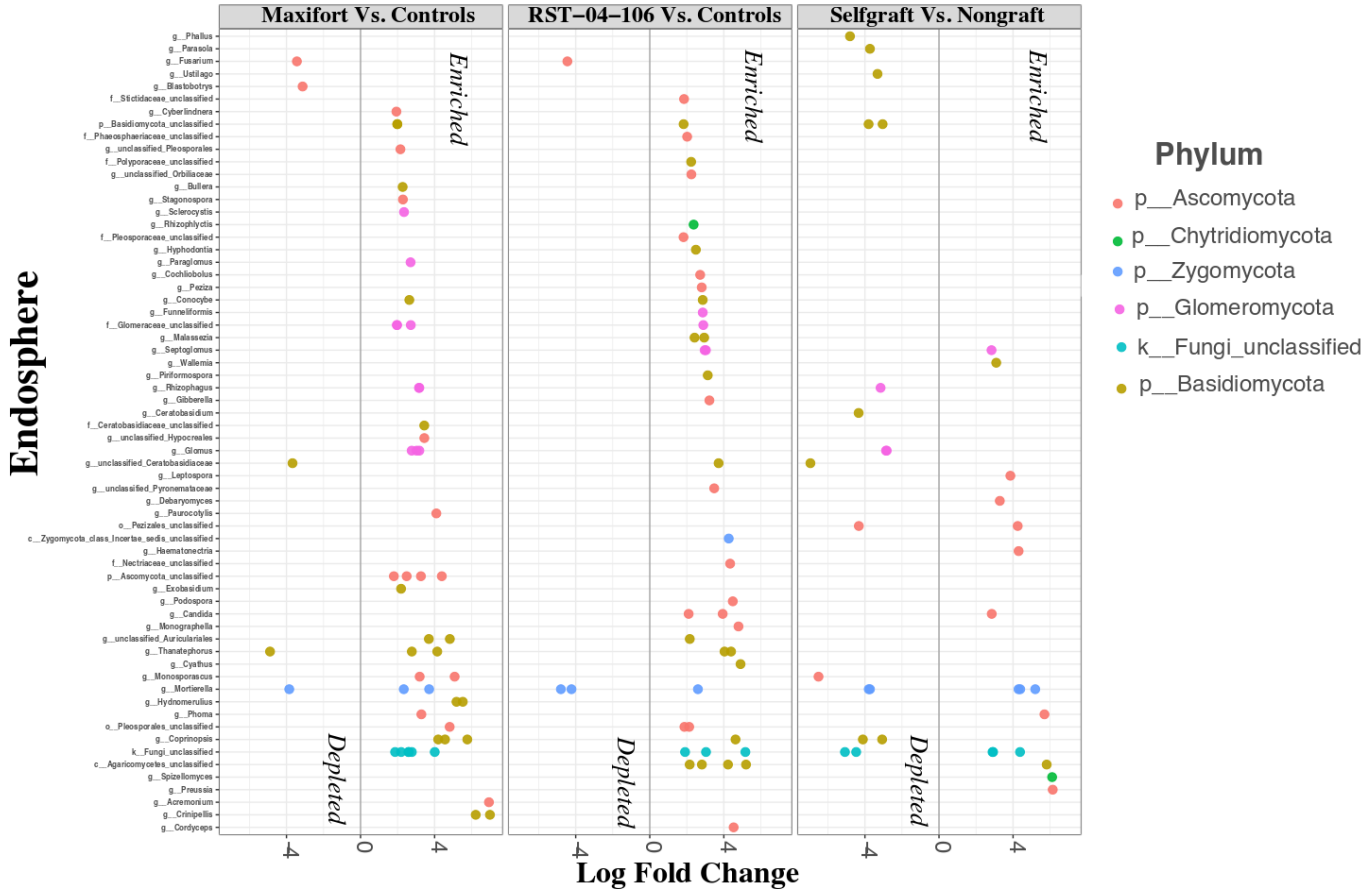

857

858 **FIG 2** Enriched and depleted OTUs across tomato rootstock genotype combinations (nongraft
859 BHN589, selfgraft BHN589, and BHN589 grafted on two hybrid rootstocks (RST-04-106 and
860 Maxifort)) evaluated for the rhizosphere (A) and the endosphere (B), using OTU counts from
861 selfgrafts and nongrafts as controls. All the tests were adjusted to control the false discovery rate
862 (FDR, $p < 0.01$) using the Benjamini-Hochberg method. Each point represents an OTU labeled at
863 the genus level and colored based on phylum, and the position along the x-axis represents the
864 abundance fold-change contrast with controls (except for the selfgraft vs. nongraft comparison,
865 where the nongraft treatment was used as a control for the contrast).

866

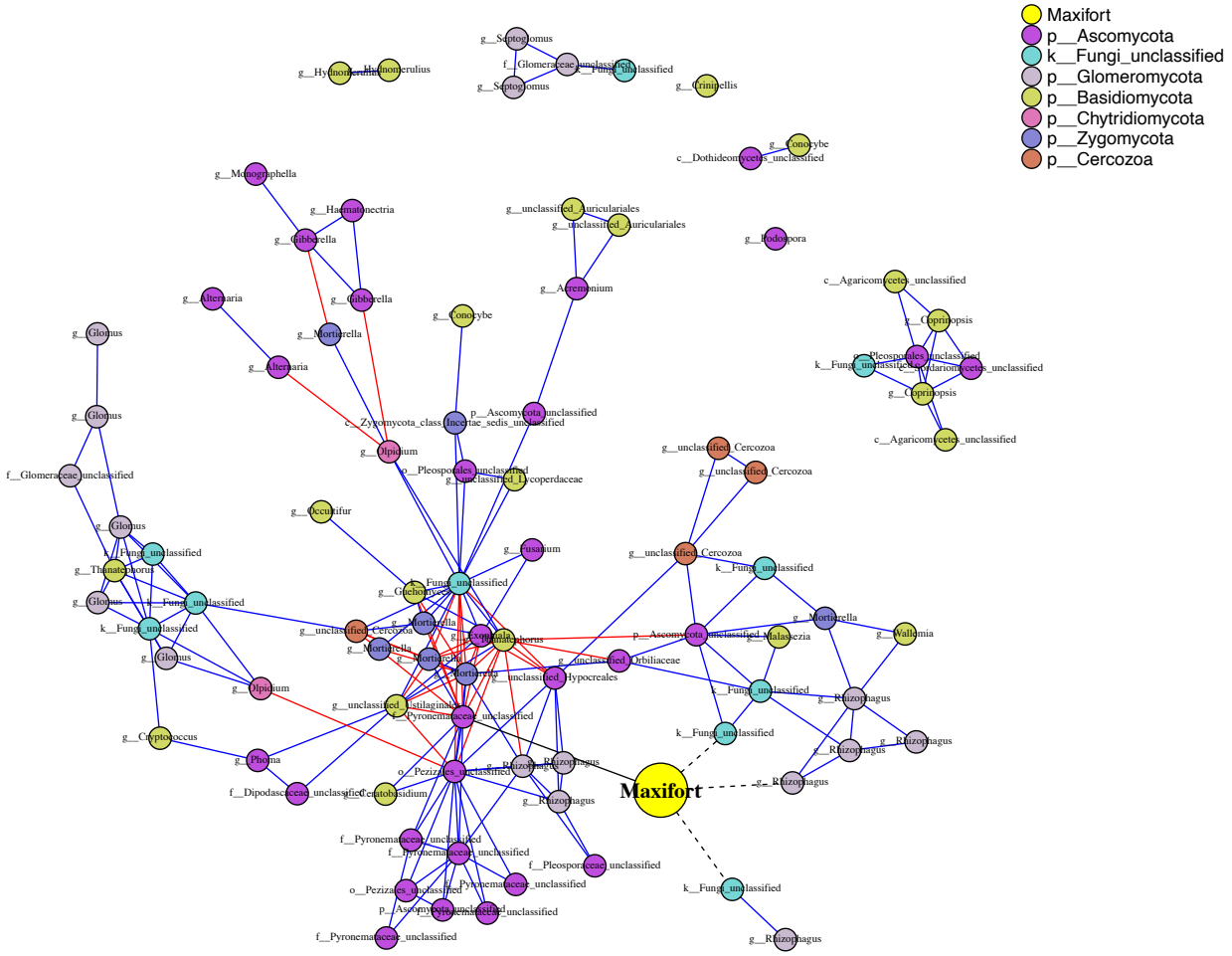

FIG 3 Phenotype-OTU network analysis (PhONA) of endosphere fungal taxa for BHN589 grafted on Maxifort. Node color indicates the phylum, except that the yellow-color node represents yield associated with the rootstock. Nodes connected to the rootstock yield node with black links are taxa that were predictive of rootstock yield, where dotted and solid lines indicate negative and positive associations with the yield node, respectively. Red and blue links represent negative and positive associations, respectively, between OTUs. Nodes are labeled with the finest-resolution taxonomic categorization available.

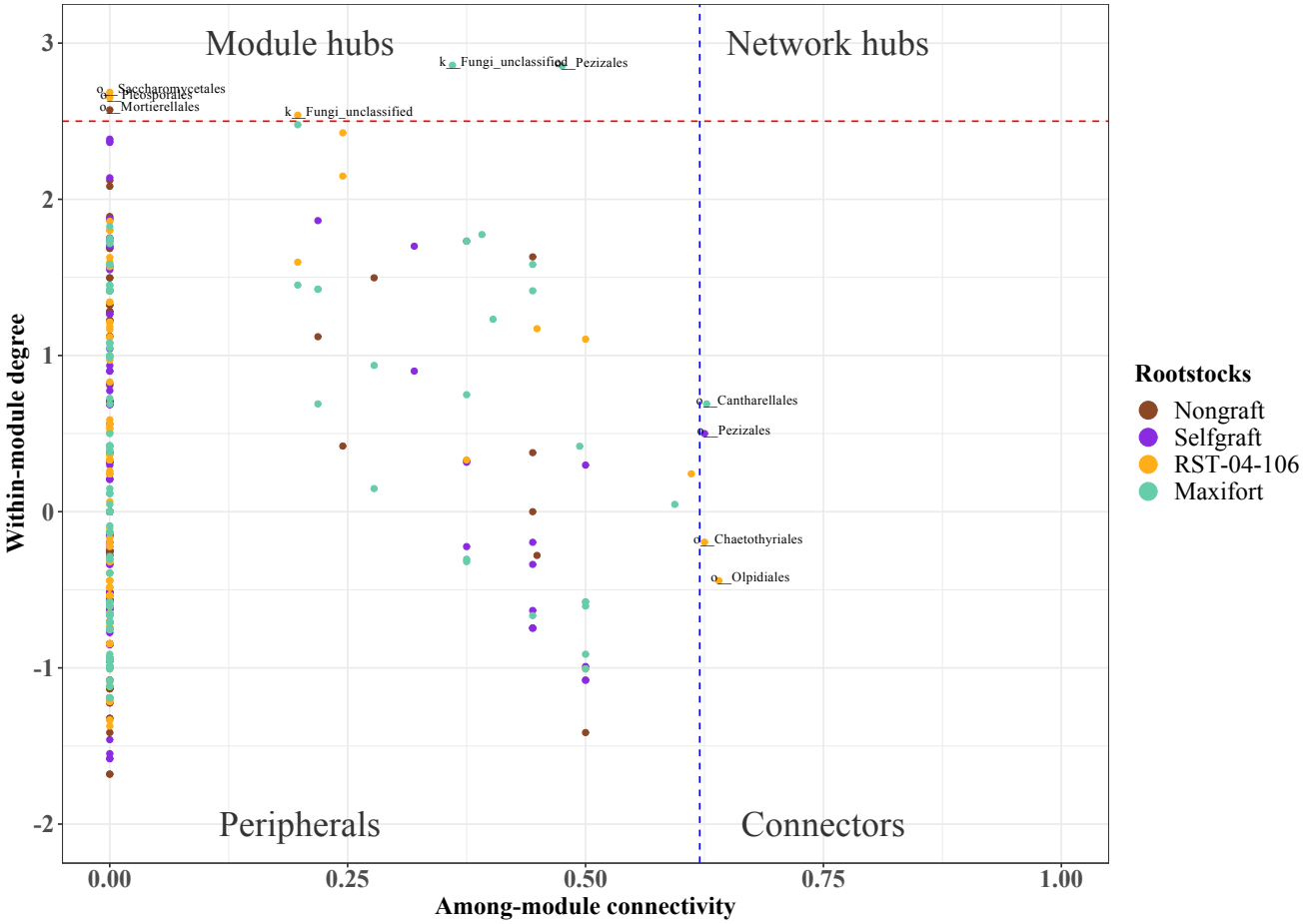

FIG 4 Partitioning of endosphere fungal OTUs according to their network roles. Nodes were divided into four categories based on within-module degree and among-module connectivity. The blue dashed line represents a threshold value (0.62) for among-module connectivity, and the red dashed line represents a threshold value (2.5) for within-module degree. Nodes were categorized as peripherals, connectors, module hubs, and network hubs. Node color indicates rootstock treatment (nongraft BHN589, selfgraft BHN589, and BHN589 grafted on two hybrid rootstocks (RST-04-106 and Maxifort)).

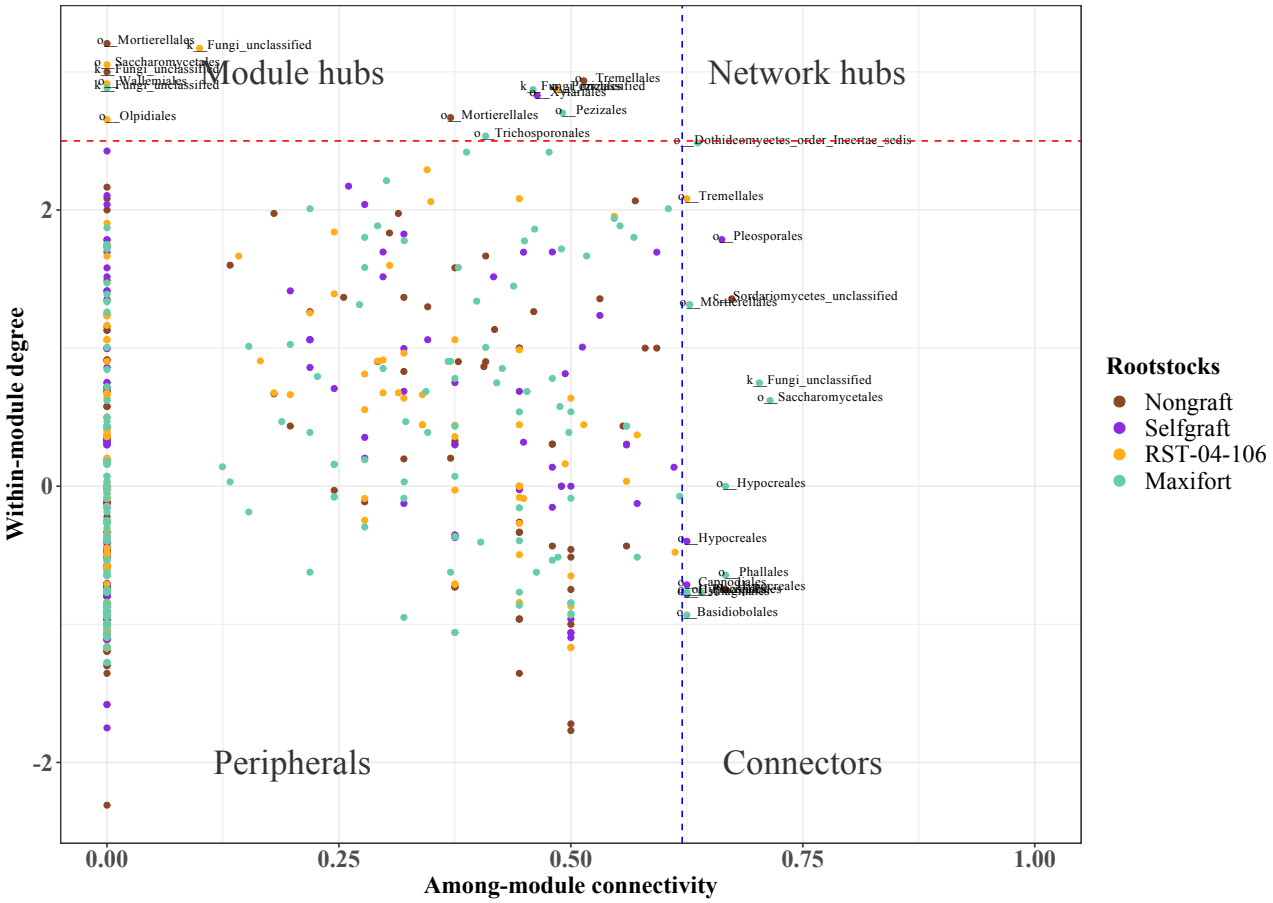

FIG 5 Partitioning of rhizosphere fungal OTUs according to their network roles. Nodes were divided into four categories based on within-module degree and among-module connectivity. The blue dashed line represents a threshold value (0.62) for among-module connectivity, and the red dashed line represents a threshold value (2.5) for within-module degree. Nodes were categorized as peripherals, connectors, module hubs, and network hubs. Node color indicates rootstock treatment (nongraft BHN589, selfgraft BHN589, and BHN589 grafted on two hybrid rootstocks (RST-04-106 and Maxifort)).

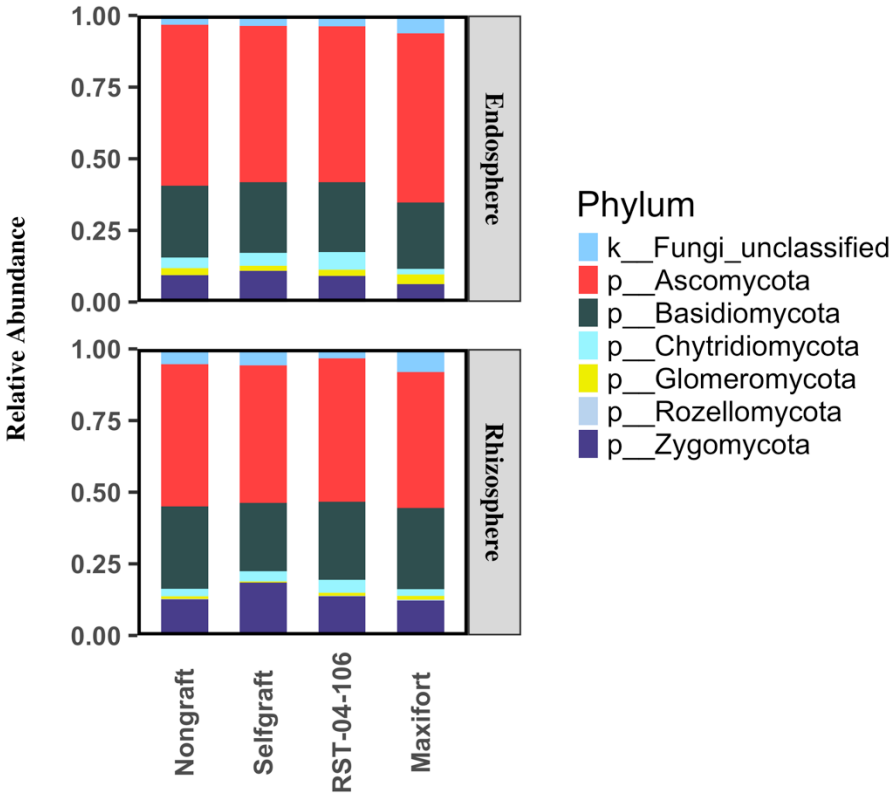

FIG S1 Relative abundance of endosphere and rhizosphere fungi at the phylum level recovered from four tomato rootstock treatments: nongraft BHN589, selfgraft BHN589, and BHN589 grafted on two hybrid rootstocks (RST-04-106 and Maxifort). Each individual bar represents a rootstock treatment, and the colored area within the bar represents the relative abundance of the corresponding phylum.

908 (A)

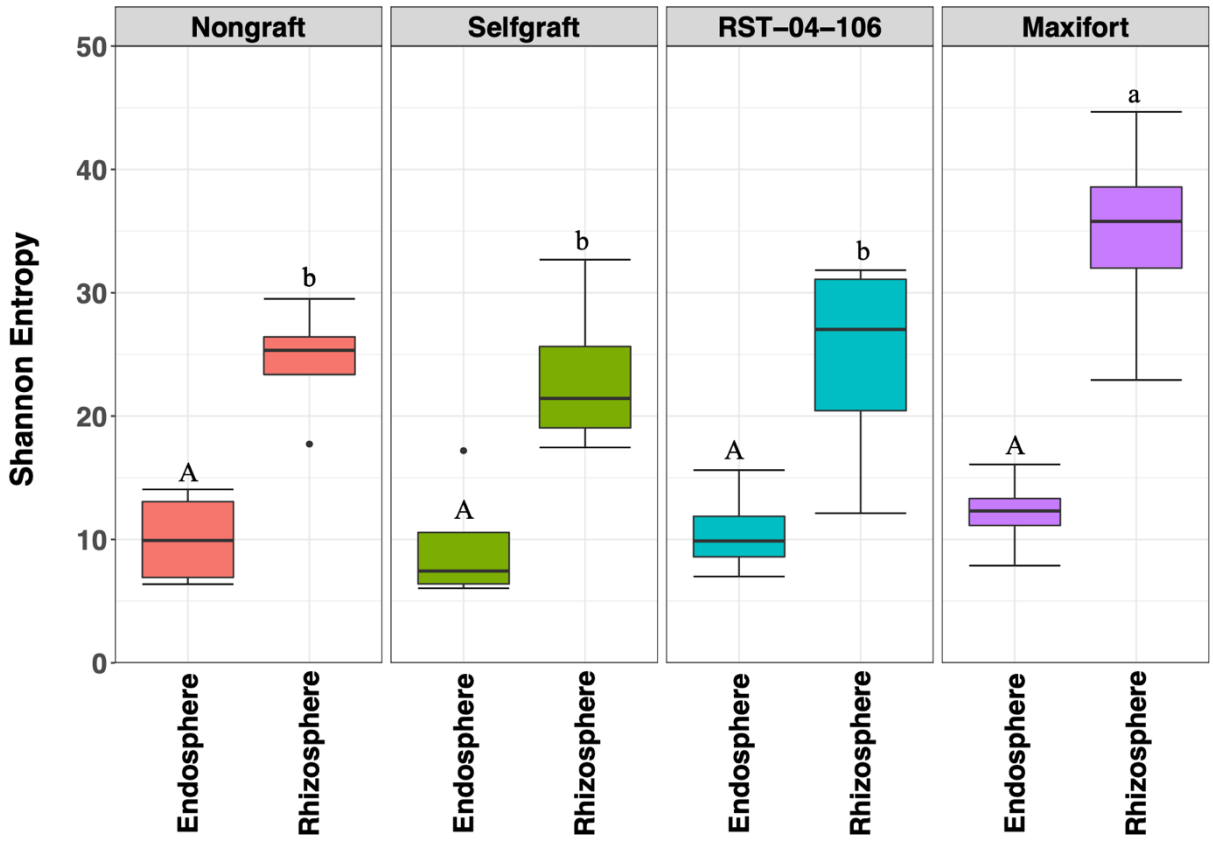
Nongraft
Selfgraft
RST−04−106
Maxifort
Shannon Entropy
50
40
30
20
10
0
A
b
A
b
A
b
A
a
Endosphere
Rhizosphere
Endosphere
Rhizosphere
Endosphere
Rhizosphere
Endosphere
Rhizosphere

909

910

911 (B)

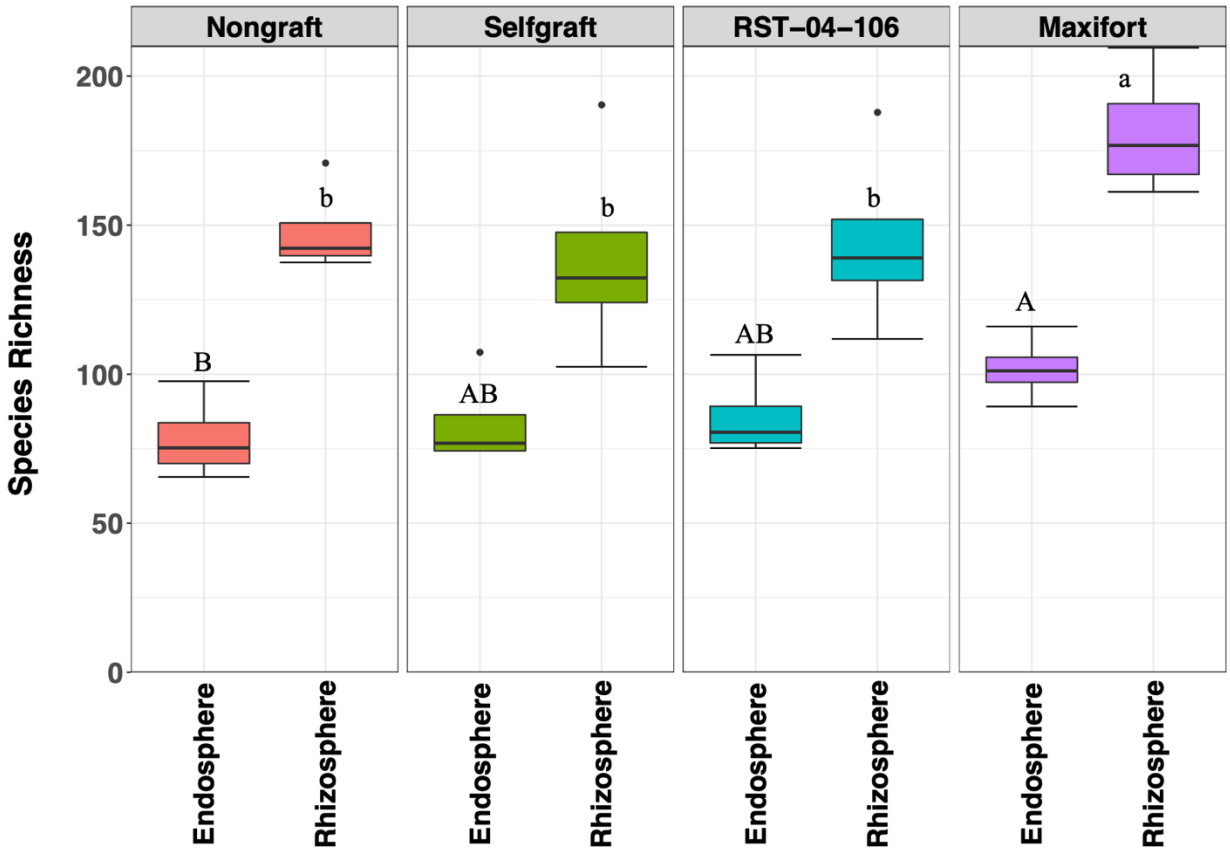

912

913

914 **FIG S2** Comparison of overall fungal diversity (A) and richness (B) associated with tomato

915 rootstock genotypes and controls, evaluated in the endosphere and rhizosphere. The plot is

916 divided by the four tomato rootstock treatments: nongraft BHN589, selfgraft BHN589, and

917 BHN589 grafted on two hybrid rootstocks (RST-04-106 and Maxifort). Shannon entropy and

918 species richness, measures of community diversity, were both higher for Maxifort ($p < 0.005$)

919 compared to the self-graft and RST-04-106 in the rhizosphere, while there was not evidence for a

920 difference in Shannon entropy in the endosphere ($p = 0.634$). Treatment means were separated

using the "difflsmeans" function as specified in the lmerTest package in R. Tests for boxplots sharing a letter or letter case type had $p > 0.05$.

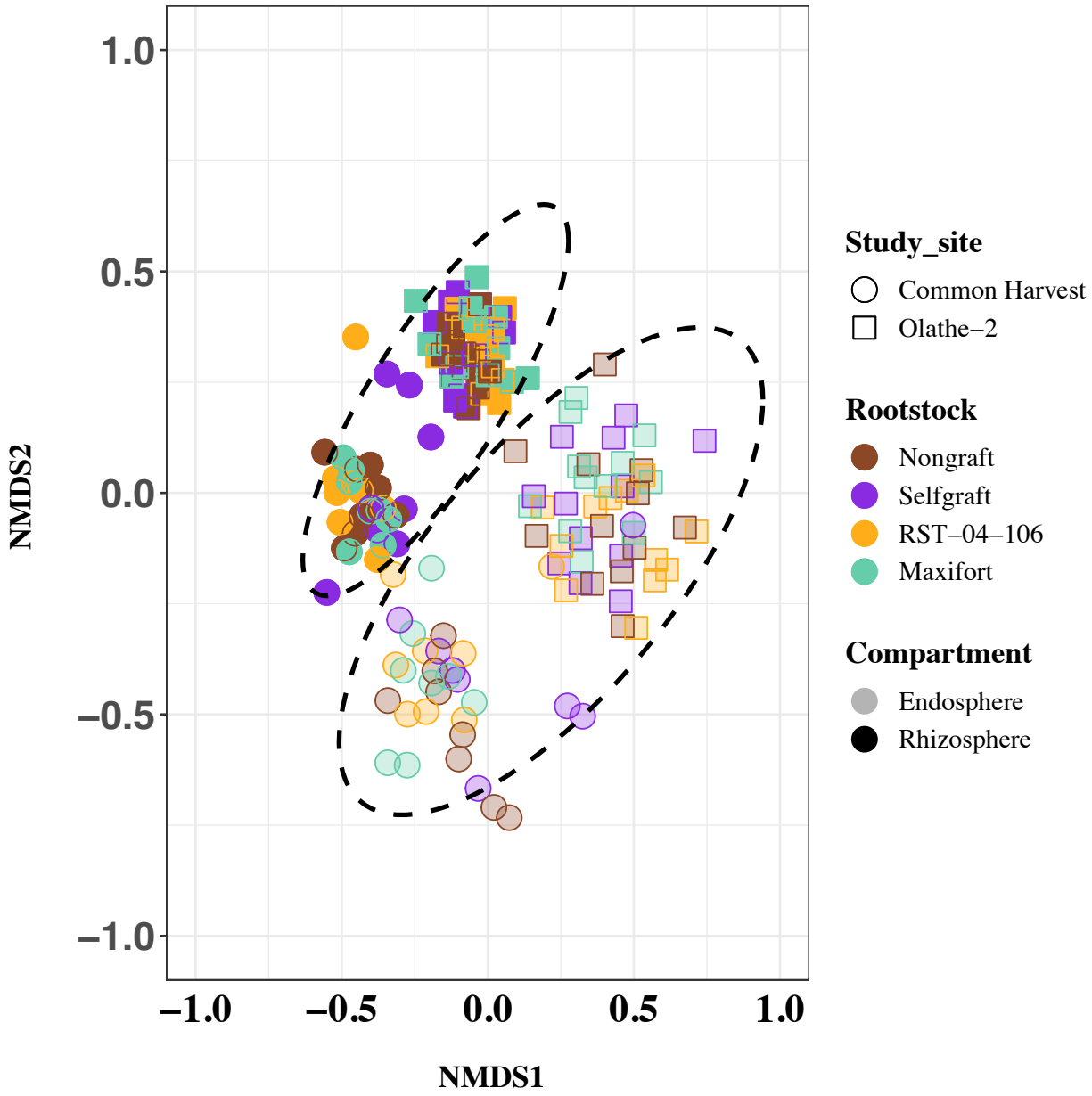

FIG S3 Non-metric multidimensional scaling (NMDS) ordination plot of samples labeled by tomato rootstock (nongraft BHN589, selfgraft BHN589, and BHN589 grafted on two hybrid rootstocks (RST-04-106 and Maxifort)), compartment (endosphere or rhizosphere), and study site, based on the Bray-Curtis dissimilarity distance matrix of fungal OTUs. Color indicates rootstock treatment, shape indicates study site, and size indicates compartment. Ellipses

931 surrounding the samples indicate the 95% CI of the endosphere and rhizosphere sample

932 centroids.

933

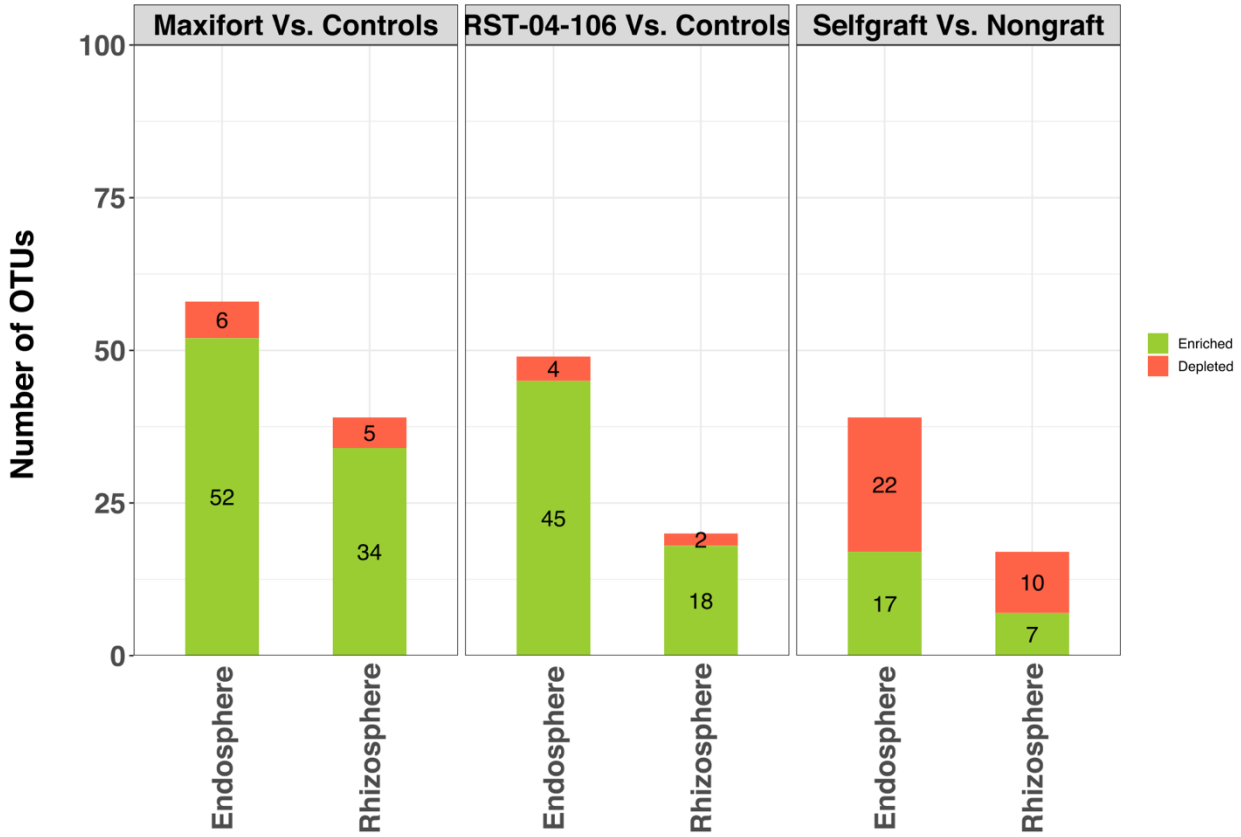

FIG S4 Number of DAOTUs in a contrast analysis, evaluated for the endosphere and rhizosphere compartments for four tomato rootstock treatments: nongraft and selfgraft BHN589, and BHN589 grafted on two hybrid rootstocks (Maxifort and RST-04-106). The green color in each bar represents the number of enriched taxa, and the red color represents the number of depleted taxa. The number of differentially changed taxa was greater for the endosphere than for the rhizosphere. Among the contrast pairs, hybrid rootstocks had a greater number of enriched taxa compared to depleted taxa. However, the number of depleted taxa was higher compared to enriched taxa in the controls. Among the treatments, Maxifort had the highest number of DAOTUs in both compartments.

A)

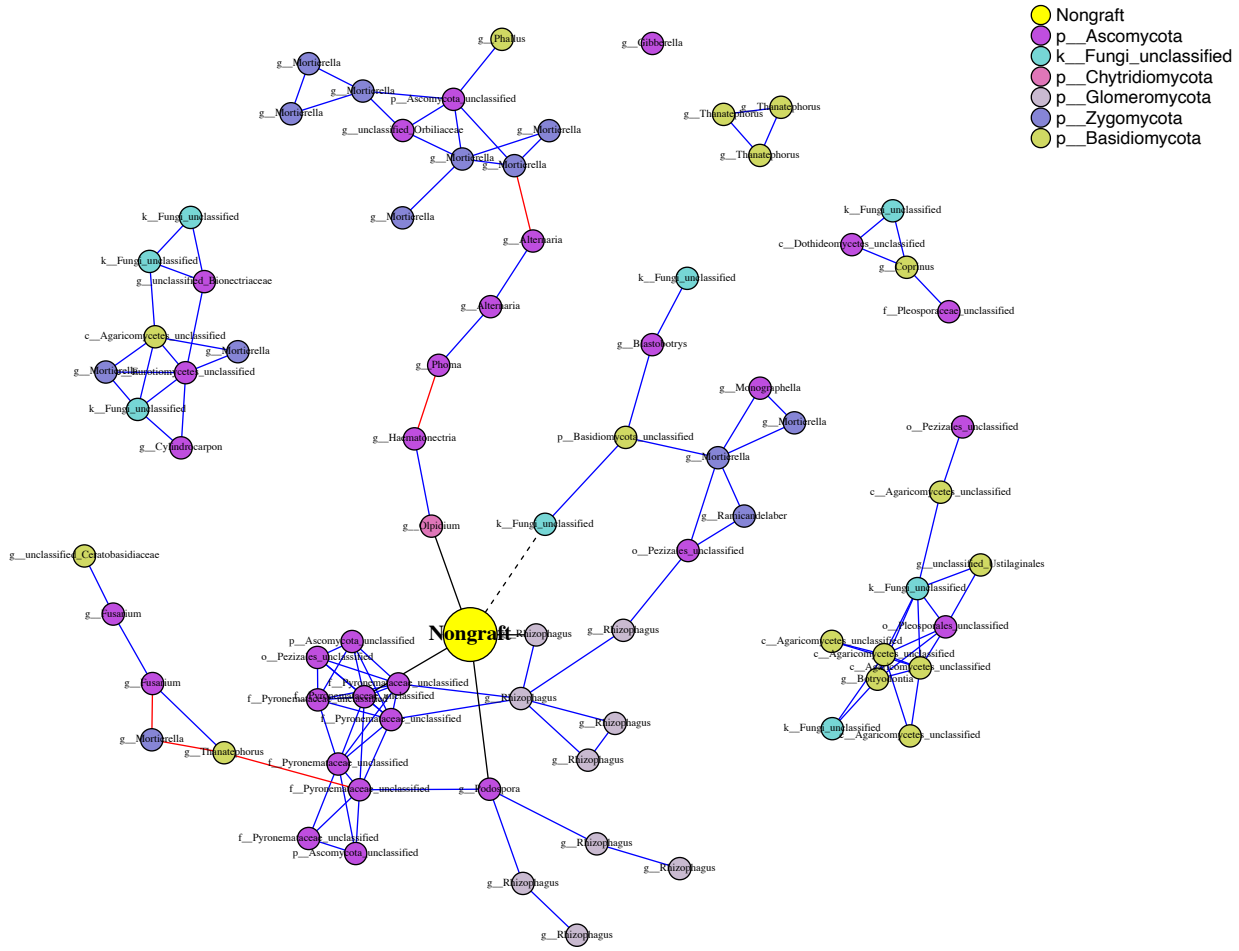
Nongraft
p__Ascomycota
k__Fungi_unclassified
p__Chytridiomycota
p__Glomeromycota
p__Zygomyota
p__Basidiomycota
Nongraft

B)

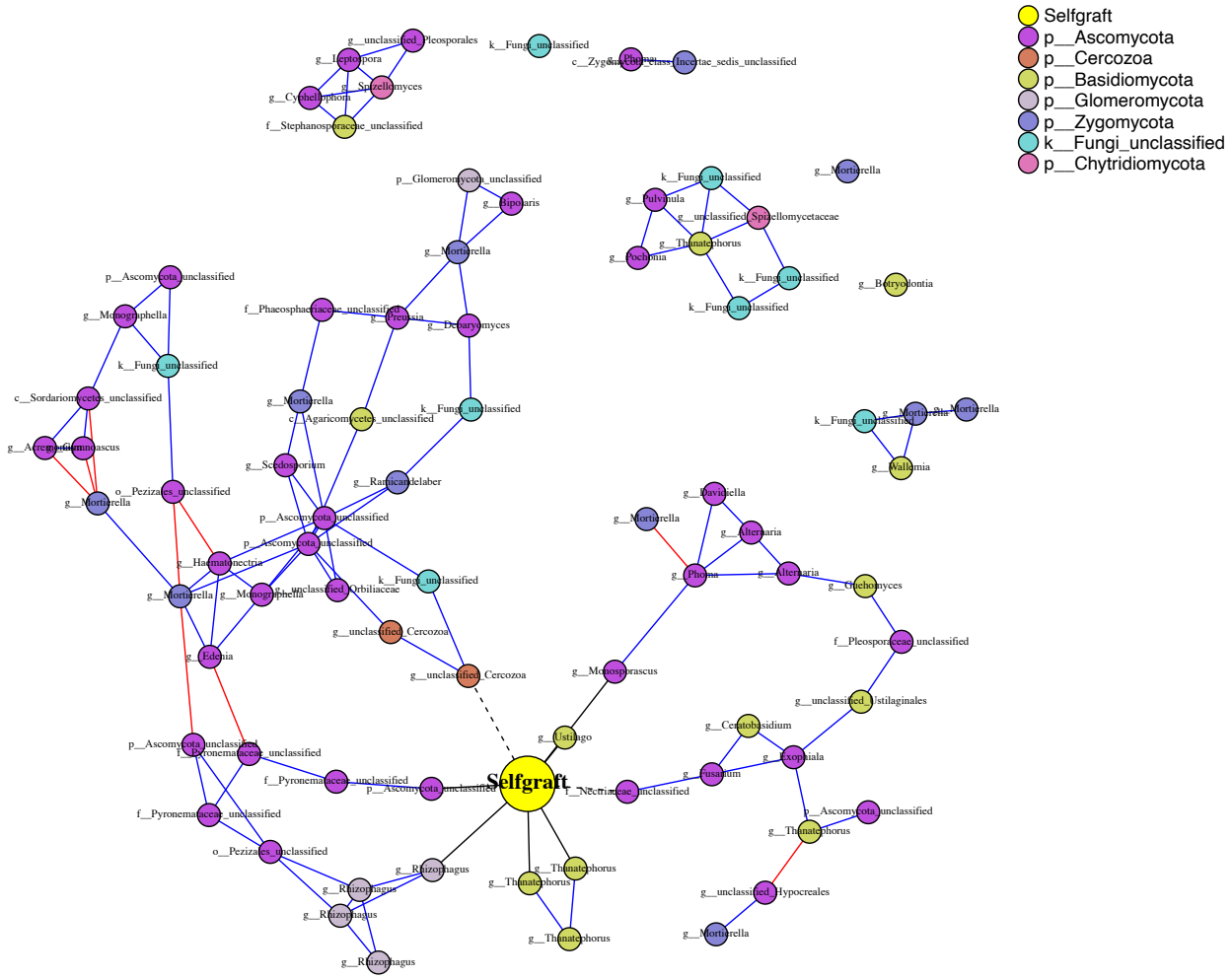
Selfgraft
p__Ascomycota
p__Cercozoa
p__Basidiomycota
p__Glomeromycota
p__Zygomycota
k__Fungi_unclassified
p__Chytridiomycota
Selfgraft

C)

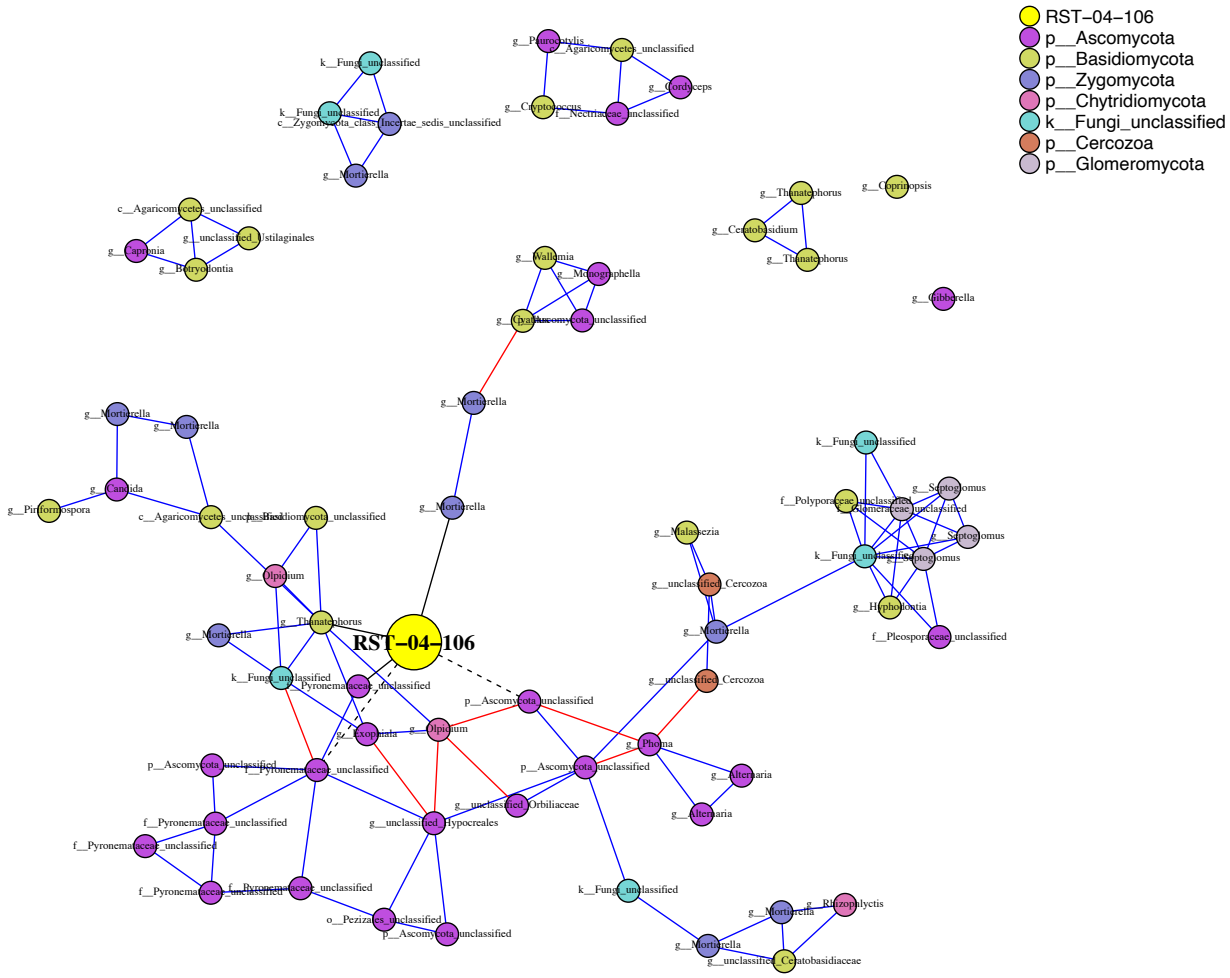

FIG S5 Phenotype-OTU network analysis (PhONA) of **endosphere** fungal taxa for tomato rootstock treatments: (A) nongraft and (B) selfgraft BHN589, and (C) BHN589 grafted on RST-04-106. Node color indicates the phylum, except that the yellow-color node represents yield associated with the rootstock. Nodes connected to the rootstock yield node with black links are taxa that were predictive of rootstock yield, where dotted and solid lines indicate negative and positive associations with the yield node, respectively. Red and blue links represent negative and positive associations, respectively, between OTUs. Nodes are labeled with the finest-resolution taxonomic categorization available.

A)

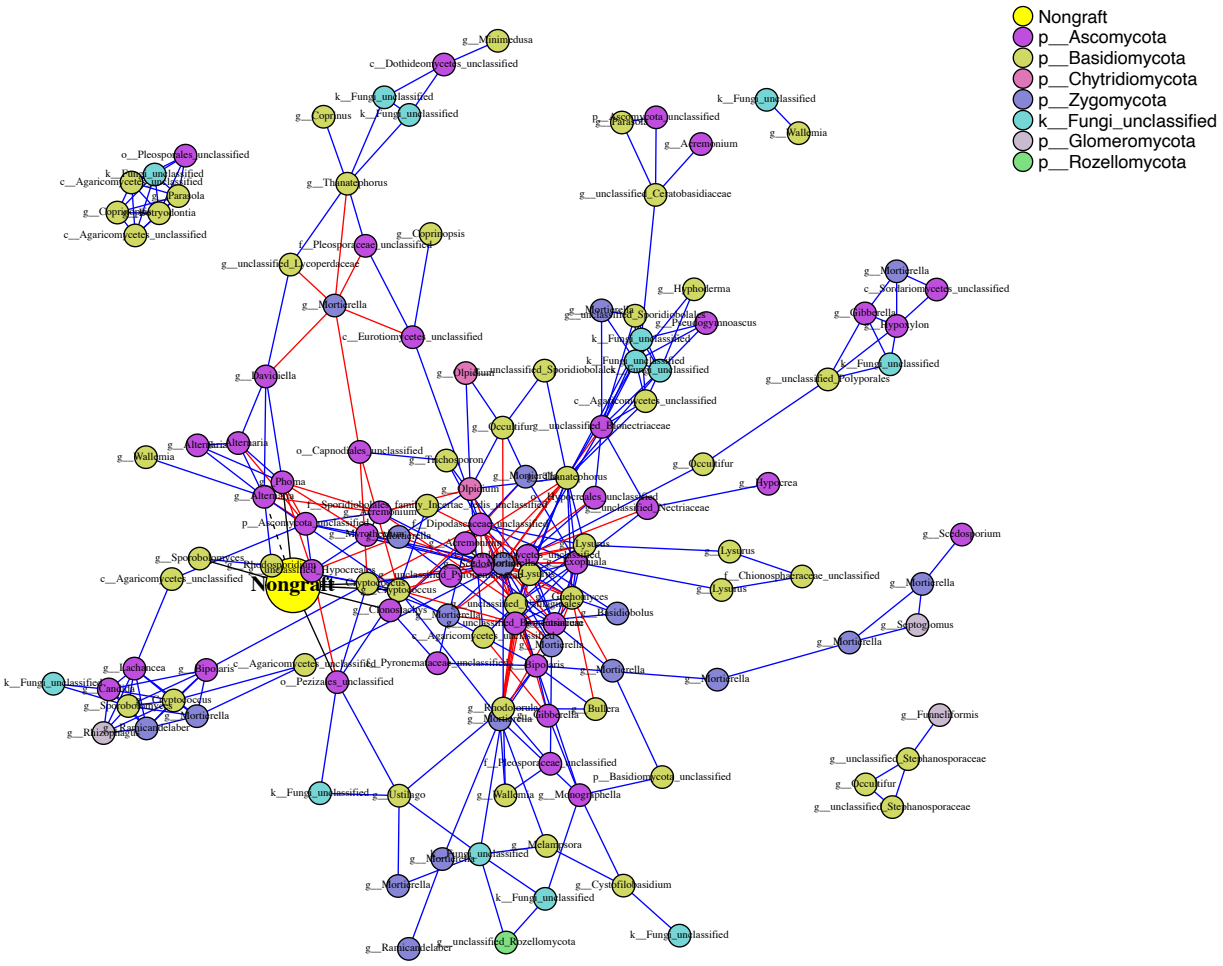
Nongraft
p__Ascomycota
p__Basidiomycota
p__Chytridiomycota
p__Zygomycota
k__Fungi_unclassified
p__Glomeromycota
p__Rozellomycota

B)

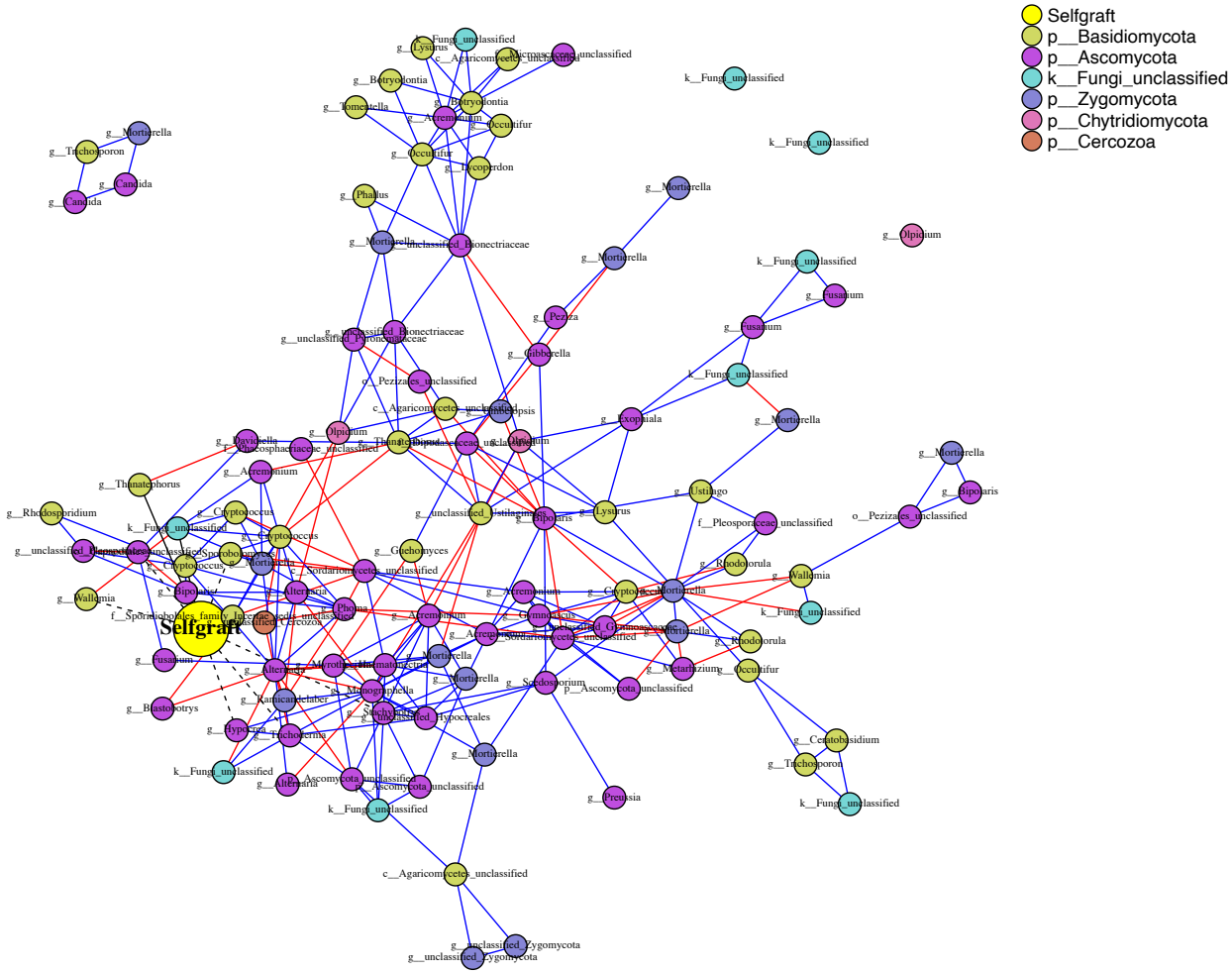
Selfgraft
p__Basidiomycota
p__Ascomycota
k__Fungi_unclassified
p__Zygomycota
p__Chytridiomycota
p__Cercozoa
Selfgraft

C)

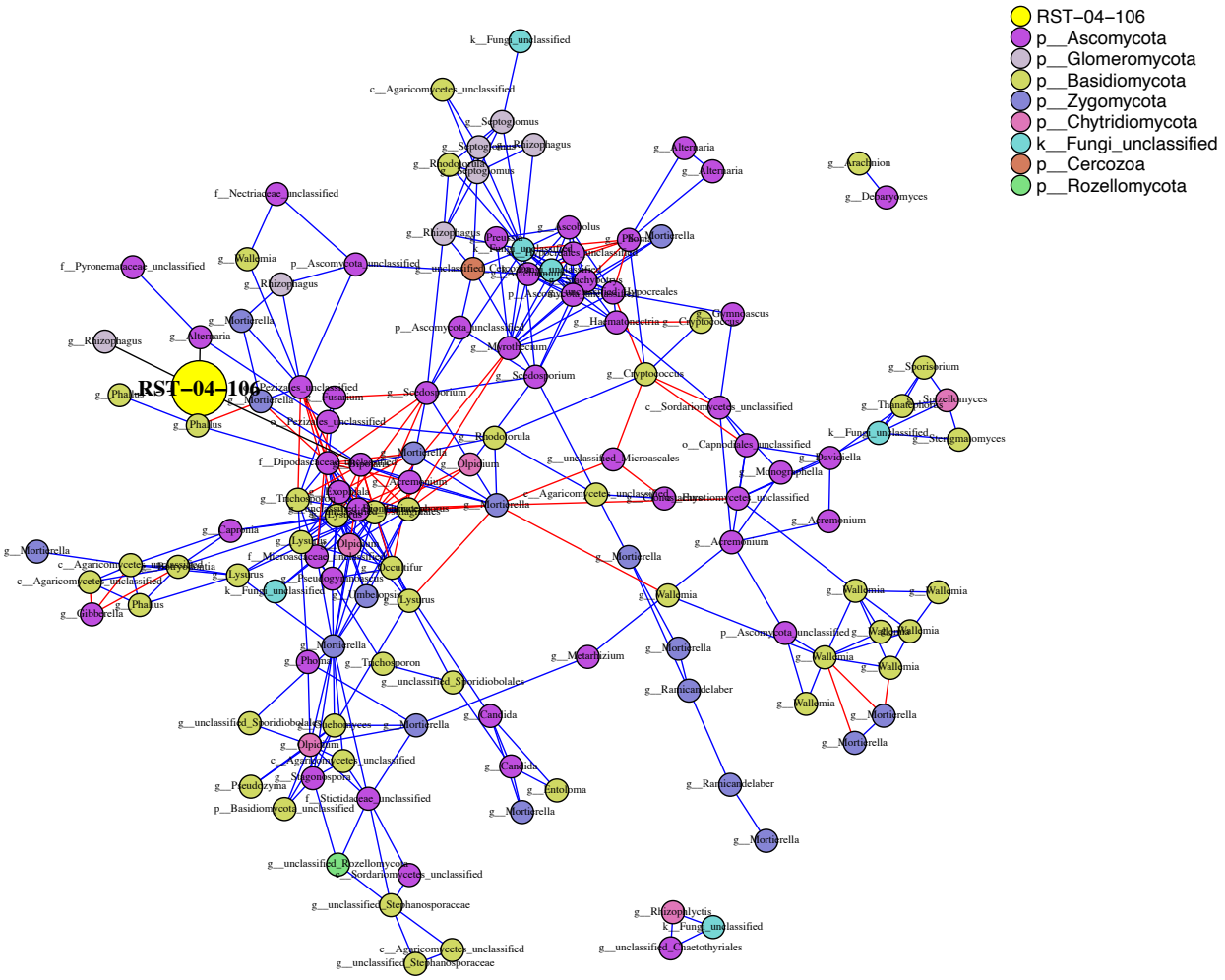
RST−04−106
p__Ascomycota
p__Glomeromycota
p__Basidiomycota
p__Zygomycota
p__Chytridiomycota
k__Fungi_unclassified
p__Cercozoa
p__Rozellomycota
RST−04−106

D)

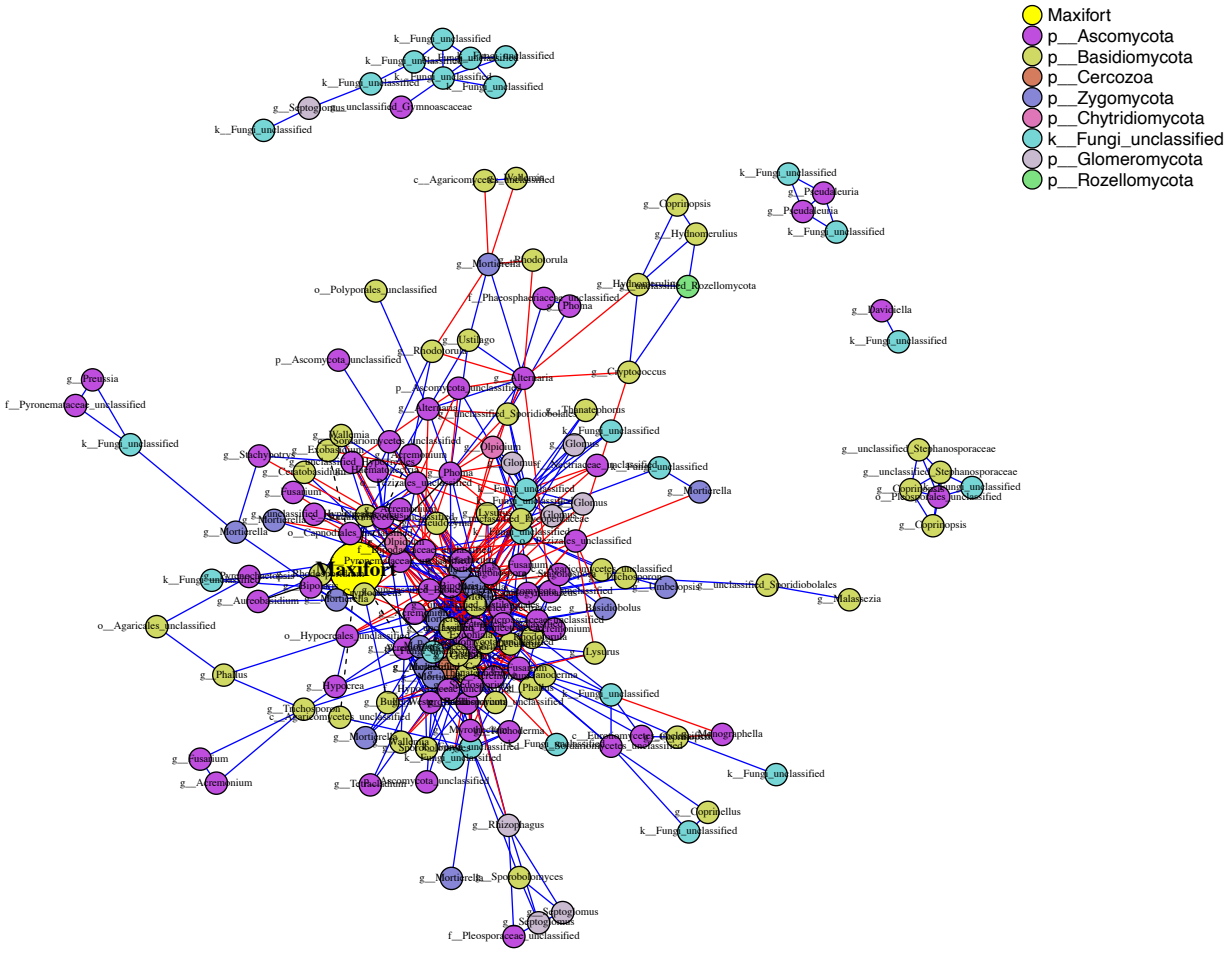

FIG S6 Phenotype-OTU network analysis (PhONA) of **rhizosphere** fungal taxa for tomato rootstock treatments: (A) nongraft and (B) selfgraft BHN589, and BHN589 grafted on two hybrid rootstocks ((C) RST-04-106 and (D) Maxifort). Node color indicates the phylum, except that the tomato-color node represents yield associated with the rootstock. Nodes connected to the rootstock yield node with black links are taxa that were predictive of rootstock yield, where dotted and solid lines indicate negative and positive associations with the yield node, respectively. Red and blue links represent negative and positive associations, respectively, between OTUs. Nodes are labeled with the finest-resolution taxonomic categorization available.

TABLE S1 Sites included in the study, their soil type, and geographic coordinates.

Study sites	Location	Latitude	Longitude	Soil type
Olathe Horticulture Research and Extension Center (OHREC)	Johnson County, KS	38.88N	94.99W	Chase silt loam
Common Harvest	Douglas County, KS	38.96N	95.20W	Eudora-Kimo complex

984 **TABLE S2** Results of the multivariate permutational analysis of variance (PERMANOVA) for
985 fungal taxon abundance data. Permutation was based on the Bray-Curtis distance matrix
986 generated for root associated fungal communities at the OTU level from four tomato rootstock
987 treatments: nongraft and selfgraft BHN589, and BHN589 grafted on two hybrid rootstocks
988 (Maxifort and RST-04-106) (1000 permutations). P values < 0.05 are in bold.

Factor	Sum of Squares	% Explained	P value
Rootstocks	1.24	2.07	**< 0.01**
Compartment	5.36	8.92	**< 0.001**
Study_Site	5.01	8.34	**< 0.001**
Year	3.23	5.38	**< 0.001**
Rootstocks:Compartment	0.58	0.97	0.972
Rootstocks:Study_Site	1.39	2.32	**< 0.01**
Compartment:Study_Site	1.59	2.65	**< 0.001**
Rootstocks:Year	1.00	1.66	0.111
Compartment:Year	1.00	1.66	**< 0.001**
Study_Site:Year	1.46	2.43	**< 0.001**
Rootstocks:Compartment:Study_Site	0.55	0.91	0.998
Rootstocks:Compartment:Year	0.49	0.82	1.000
Rootstocks:Study_Site:Year	1.22	2.03	**< 0.01**
Compartment:Study_Site:Year	0.60	1.00	**< 0.01**
Rootstocks:Compartment:Study_Site:Year	0.60	1.00	0.989
Residuals	34.75	57.86	
Total	60.07	100.01	

989

TABLE S3 Network attributes and links observed in the fungal association networks for four tomato rootstock treatments: nongraft and selfgraft BHN589, and BHN589 grafted on two hybrid rootstocks (Maxifort and RST-04-106) in each of rhizosphere and endosphere compartments.

Compartment	Rootstocks	N	Node	Edge	Node Degree	Density	Modules (SA)	Negative Edge	Po E
Endosphere	Nongraft	20	78	112	1.6	0.04	10	5	
	Selfgraft	20	115	115	1.4	0.04	11	9	
	RST-04-106	20	71	110	1.5	0.04	11	9	
	Maxifort	20	92	182	2.0	0.04	10	32	
Rhizosphere	Nongraft	20	132	337	2.6	0.04	12	72	
	Selfgraft	20	113	272	2.4	0.04	9	63	
	RST-04-106	20	133	338	2.5	0.04	11	54	
	Maxifort	20	173	740	4.3	0.04	11	279	